Bioactive Materials 21 (2023) 157–174

Contents lists available at ScienceDirect

Bioactive Materials

journal homepage: www.keaipublishing.com/en/journals/bioactive-materials

Review article

Recent advances in engineered polymeric materials for efficient photodynamic inactivation of bacterial pathogens

Sathishkumar Gnanasekar [a], Gopinath Kasi [a], Xiaodong He [a], Kai Zhang [a], Liqun Xu [a,b,*], En-Tang Kang [a,c,**]

[a] Chongqing Key Laboratory for Advanced Materials and Technologies of Clean Energies, School of Materials and Energy, Southwest University, Chongqing, 400715, PR China

[b] Key Laboratory of Laser Technology and Optoelectronic Functional Materials of Hainan Province, College of Chemistry and Chemical Engineering, Hainan Normal University, Haikou, 571158, PR China

[c] Department of Chemical and Biomolecular Engineering, National University of Singapore, Kent Ridge, 117576, Singapore

ARTICLE INFO

Keywords:
Antibacterial photodynamic therapy
Polymers
Photosensitizers
Conjugation
Hydrogels
Biomaterials

ABSTRACT

Nowadays, infectious diseases persist as a global crisis by causing significant destruction to public health and the economic stability of countries worldwide. Especially bacterial infections remain a most severe concern due to the prevalence and emergence of multi-drug resistance (MDR) and limitations with existing therapeutic options. Antibacterial photodynamic therapy (APDT) is a potential therapeutic modality that involves the systematic administration of photosensitizers (PSs), light, and molecular oxygen (O_2) for coping with bacterial infections. Although the existing porphyrin and non-porphyrin PSs were effective in APDT, the poor solubility, limited efficacy against Gram-negative bacteria, and non-specific distribution hinder their clinical applications. Accordingly, to promote the efficiency of conventional PSs, various polymer-driven modification and functionalization strategies have been adopted to engineer multifunctional hybrid phototherapeutics. This review assesses recent advancements and state-of-the-art research in polymer-PSs hybrid materials developed for APDT applications. Further, the key research findings of the following aspects are considered in-depth with constructive discussions: i) PSs-integrated/functionalized polymeric composites through various molecular interactions; ii) PSs-deposited coatings on different substrates and devices to eliminate healthcare-associated infections; and iii) PSs-embedded films, scaffolds, and hydrogels for regenerative medicine applications.

1. Introduction

An increased outbreak of bacterial infectious diseases has become a severe life-threatening health concern worldwide due to increasing mortality and catastrophic consequences [1]. Since the 1930s, many prophylactic antibiotic medications have been discovered and practiced to suppress (bacteriostatic) or kill (bactericidal) harmful bacterial strains. Each antibiotic has its actions, including cell wall targeting, protein and nucleic acid synthesis inactivation, and inhibition of enzyme production [2]. Although these antibiotics saved millions of lives, indiscriminate misuse or overuse inevitably worsened their effectiveness and posed an economic burden due to the rise of MDR bacteria or superbugs [3]. MDR is associated with planktonic bacteria's physiological adaptation and gene mutation to form an extracellular (EC)

Abbreviations: APDT, Antibacterial photodynamic therapy; PSs, Photosensitizers; $^1O_2$, Singlet oxygen; APTT, Antibacterial photothermal therapy; PDI, Photodynamic inactivation; ROS, Reactive oxygen species; Hp, Hematoporphyrin; Ce6, Chlorin e6; MRSA, Methicillin-resistant *Staphylococcus aureus*; BODIPY, Boron dipyrromethene; RB, Rose bengal; MB, Methylene blue; CUR, Curcumin; HYP, Hypocrellin; ICG, Indocyanine green; PCL, Poly(ε-caprolactone); CS, Chitosan; PEI, Polyethylamine; PPIX, Protoporphyrin IX; PEG, Poly(ethylene glycol); PDA, Polydopamine; PVA, Poly(vinyl alcohol); CV, Crystal violet; α-CD, α-cyclodextrin; BP, Black phosphorus.

Peer review under responsibility of KeAi Communications Co., Ltd.

* Corresponding author. Chongqing Key Laboratory for Advanced Materials and Technologies of Clean Energies, School of Materials and Energy, Southwest University, Chongqing, 400715, PR China.

** Corresponding author. Chongqing Key Laboratory for Advanced Materials and Technologies of Clean Energies, School of Materials and Energy, Southwest University, Chongqing, 400715, PR China.

E-mail addresses: xulq@swu.edu.cn (L. Xu), cheket@nus.edu.sg (E.-T. Kang).

https://doi.org/10.1016/j.bioactmat.2022.08.011
Received 9 May 2022; Received in revised form 3 August 2022; Accepted 11 August 2022

matrix, including new variant biofilm formation [4]. The world health organization study reported that "antibiotic resistance is no longer a prediction for the future, it is happening right now across the world", which created a high alarm among the research fraternity [5]. As reported by the Centers for Disease Control and Prevention, antibiotic resistance became a global crisis due to poor sanitation, lack of rapid diagnosis, and antibiotic abuse [6]. The persistence of this situation could cause the death of nearly 10 million people/year by 2050, which is a larger mortality figure than cancer [7]. The foregoing facts deliberate that the world has entered a critical time, and invasive infectious agents are difficult to control by existing treatment modalities. Therefore, developing novel engineered materials for antibacterial therapeutic ventures without MDR is mandatory to normalize the rising epidemic or pandemic.

Phototherapeutic options, such as APDT and antibacterial photothermal therapy (APTT), are recognized as potent weapons to combat bacterial infections [8–13]. APTT requires a powerful photothermal agent to convert photon energy into heat and kill bacteria via hyperthermia [12]. APDT is an interactive technology that operates with PSs and holds the ability to eradicate/inhibit bacterial growth by generating reactive oxygen species (ROS) under light irradiation [14]. Recently, both MDR and non-MDR bacterial pathogens have been shown to be vulnerable to APDT [15,16]. As a result, researchers around the globe have given scrupulous attention to biocompatible polymers in combination with active PSs for photo-induced effective bacterial eradication. Engineering of PSs incorporated polymeric functional materials increases their efficacy as well as integrates multimodal therapy modalities. These multifunctional platforms can have many advantages, including (i) site-specific localized PSs delivery with high selectivity and minimal side effects; (ii) improving the photostability of PSs and protecting them from degradation; (iii) stimuli-responsive bacterial-killing strategies for long-term action in complex microenvironment; (iv) targeting and penetrating bacterial cell membrane; and (v) enhancing PSs' bactericidal action against Gram-negative bacteria.

This review predominantly summarizes the photodynamic inactivation (PDI) properties of PS-polymer hybrid systems. Firstly, we have reexamined the limitations of conventional porphyrin and non-porphyrin-based PSs in APDT. Furthermore, the advantages of PS-polymer's combinational formulations for treating bacterial infections were emphasized. Finally, the efficiencies of several engineered polymeric biomaterials in APDT, such as composites, surface coatings, films, scaffolds, and hydrogels, as well as their biomedical possibilities, were addressed. Thus, the present review aimed to i) comparatively summarize the recent improvement in polymer-based APDT formulations, ii) explicitly present their preparation and physio-chemical features, and iii) deliberate their applicability in future clinical translation.

2. Antibacterial photodynamic therapy

Photodynamic therapy (PDT) is a non-invasive, clinically approved and safe therapeutic strategy. Although light-based therapeutic modalities have existed since ancient times, a booming interest has ensued after conceiving the term "Photodynamic Action" by von Tappeiner [17]. Over the past 100 years, this therapeutic venture has been explored mainly in various health care disciplines, such as trauma care, dermatology, gynaecology, oncology, and urology [18,19]. APDT is an intriguing non-systemic option for effectively killing bacterial pathogens that are recalcitrant to standard drugs. The concept of APDT for bacterial elimination evolved in the mid-1990s, which is a non-antibiotic and surgery-free process with relatively minimized side effects [20]. The PSs, light sources, and molecular oxygen are three fundamental prerequisites for APDT. Combining these three components in the right proportions triggers a chain of reactions to induce bacterial death, particularly against MDR bacteria [21,22].

The APDT received a booming interest after discovering "light-activated dyes" also known as PSs, which absorb light with a particular wavelength, resulting in photochemical or photophysical reactions. Numerous strategies have been used over the past two decades to increase the PDI activity of PSs by chemical modifications or synthesizing novel PS derivatives [23]. In addition to the unique photophysical characteristics, an ideal PS for APDT should possess high purity, solubility/dispersibility, stability, biocompatibility, high ROS yield, light-absorbing capacity (600–800 nm), stable triplet state, and low aggregation tendency [24,25]. Porphyrin-based PSs are well-known fluorescent pigments that ubiquitously exist in living systems and actively participate in significant bioactivities, such as photosynthesis (chlorophylls, Chls), electron transfer (cytochromes), and oxygen transport (heme group) [26]. The porphyrin PSs can be further categorized into first-generation (hematoporphyrin (Hp) derivatives, Photofrin®, and Photogem®) and second-generation (chlorin e6 (Ce6), bacteriochlorin, protoporphyrin IX (PPIX), and phthalocyanine derivatives) PSs [27,28]. Based on their photophysical and chemical properties, the non-porphyrin PSs are classified as synthetic dyes (phenothiazines, xanthenes, and boron-dipyrromethenes (BODIPYs)), natural PSs, and nanomaterials (NMs)-based PSs [29–33]. These PSs have gained much attention for their strong absorbance in the phototherapeutic window (600–800 nm) [34] and high ROS generation. However, the inherent limitations like solubility, ineffective against Gram-negative pathogens, and slow *in vivo* clearance rate have to be resolved for successful clinical applications [30,35].

In a typical APDT, the PS tends to absorb visible/near-infrared (NIR) photons and excites to its high-energy singlet state ($^1PS^0$) [36]. Nevertheless, the excited electron spins are unstable with a short lifetime (<1 μs). The excited molecule ($^1PS^*$) can undergo redox reactions or intersystem crossing (ISC) to produce a longer-lived triplet state ($^3PS^*$). As shown in Fig. 1a, photochemical reactions occur via Type I or Type II mechanisms with relative proximity between the $^3PS^*$ and substrate [15,37]. In Type I reaction, the $^3PS^*$ transfers an electron to a substrate, which is usually molecular oxygen, and triggers highly reactive superoxide anion ($O_2\cdot^-$) and hydroxyl radicals (·OH) production. All these ROS can induce irreparable oxidative damage to the bacterial cell membranes and other functional biomolecules like DNA, endoenzymes, proteins, and fatty acids [38,39]. The excited $^3PS^*$ reacts with molecular oxygen in Type II reaction and produces electronically highly reactive singlet oxygen ($^1O_2$) through the energy transfer ($^3PS^*\rightarrow O_2$) process. The generated $^1O_2$ holds the ability to eliminate bacterial pathogens via triggering photodynamic action, which inactivates cellular antioxidants and promotes oxidative stress-mediated cell-killing effects [40]. It was established that the Type I and Type II reactions coincide in APDT, and their ratio largely relies on the type of PSs and the microenvironment of infected sites. Compared to other therapeutic options in the literatures, APDT can quickly kill MDR bacterial pathogens [41,42]. Most importantly, the ROS released by PSs has a multi-target effect on bacterial cell structures and various metabolic pathways (Fig. 1b) [43]. Bacteria's inability to sense oxidative stress and disabling of cross-generation adaptivity make APDT less prone to bacterial resistance even after recurrent therapy [44]. For instance, the inorganic NMs such as metals [45], metal oxides [46], metal-organic frameworks (MOFs) [47], carbon dots [48], and two dimensional (2D) NMs [49,50] themselves act as PSs owing to their photon-absorption and ROS generating properties. In particular, the metal compounds like gallium (Ga) hybridized with indocyanine green (ICG) nanoparticles (NPs) have been demonstrated to eradicate MDR bacteria through PDI and iron metabolism blocking synergistically. It was noticed that the concentration of Ga (0–25 μg/mL) and dosage of laser intensity (0–1 W/cm^2) progressively inhibited the bacterial survival rate. The ICG-Ga hybrid NPs combined with NIR irradiation inhibits ≥95% of biofilm-forming bacteria as compared with the individual treatment of Ga (60%) and ICG (30%) (Fig. 1c) [51]. Thus, based on the abovementioned factors and facts, the APDT platform can be used to engineer polymeric functional materials for eliminating MDR bacterial infections in chronic wounds, implants and medical devices.

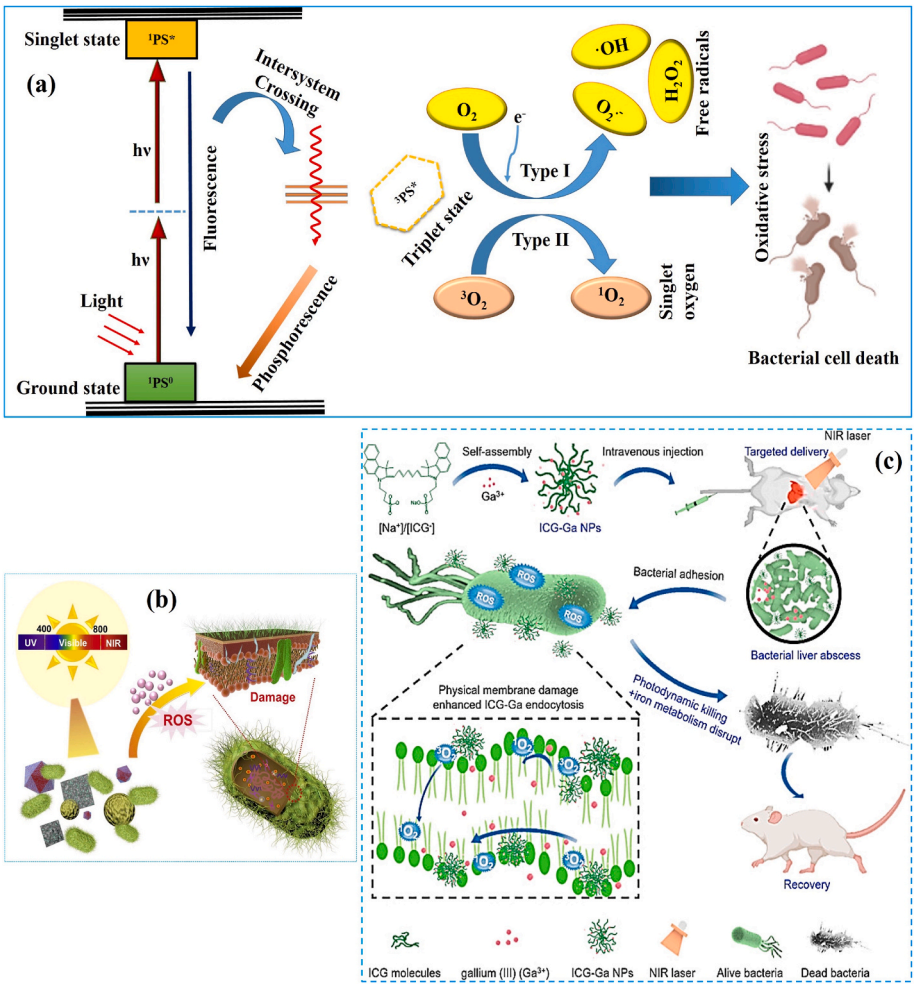

Fig. 1. (a) Illustration of Type I and Type II photochemical mechanism of APDT (Jablonski diagram). **(b)** Schematic illustration of the mechanism of bacterial damage. Reprinted with permission from Ref. [8], Copyright © 2020, Elsevier. **(c)** Schematic illustration of the synthesis of ICG-Ga NPs and their APDT action to treat infected liver abscess. Reprinted with permission from Ref. [51] Copyright © 2021, Elsevier.

3. Polymeric composites

As mentioned earlier, most reported PSs are hydrophobic with poor bioavailability, minimizing cell membrane adhesion and penetration [33,52]. Due to the short half-life of $^1O_2$ and free radicals in the biological microenvironment, the localization of PSs at the target site is critical to achieving strong APDT effects. Therefore, different strategies have been developed to increase the solubility/dispersibility and APDT efficacy of PSs against various pathogens. Accordingly, polymer-based composites were developed as ideal candidates for reinforced APDT applications mainly because of their non-toxicity, ability to mimic functional organs and lower inflammatory reactions. Besides, the polymeric matrices hold photon receiving ability and transfer excitation energy to PSs in a phenomenon known as the "antenna" effect [53]. As shown in Table 1, a plethora of natural (chitosan (CS), bacterial cellulose (BC), gelatin, and hyaluronic acid (HA)) and synthetic (polyethylamine (PEI), polystyrene (PSt), and poly(ε-caprolactone) (PCL)) polymers have been explored to synthesize various hybrid materials for APDT. The PSs were immobilized onto both natural and synthetic polymers via physical blending [54], conjugation [55], surface functionalization [56], and encapsulation [57]. Natural polymers are preferred for nanocomposite preparation due to their non-toxicity, availability, and biocompatibility. The polymer-PS composites were formed by host-guest interaction [58,59], covalent linkage [60–64] and post-loading [65] (Fig. 2a–d). In cross-linking and self-assembly-based encapsulation, the PSs were blended with a polymeric reaction mixture and physically entrapped inside the matrix through various interactions, including electrostatic, hydrogen bonding, and hydrophobic interactions [66,67]. In certain formulations, the PSs were also covalently linked with monomers to polymerize into composites [68].

3.1. Photosensitizers-integrated polymers

Natural polysaccharides can be employed to improve the affinity, biocompatibility, and dispersibility of PSs. Li et al. [55] have developed an APDT strategy for enhancing the PDI efficacy of rose bengal (RB) via conjugating with bacterial exopolysaccharide (EPS) to form negatively charged EPS-RB NPs. The EPS-RB NPs showed increased PDI action against *Escherichia coli* (*E. coli*, 8 μM) and *Staphylococcus aureus* (*S. aureus*, 500 nM) under light irradiation through increased surface affinity and $^1O_2$ generation. Other studies have focused on CS to boost the PDI efficacy of Ce6 [61,69]. Ce6 was conjugated with CS via amide linkage between the carboxyl and free amine group, forming a nano assembly (Fig. 3a). The improved cell membrane affinity and cellular uptake of polymer-PS combinations are depicted by elevated fluorescence intensity (42-fold) and surface charge (0.7 mV) (Fig. 3b–d) of CS-Ce6 treated methicillin-resistant *S. aureus* (MRSA) compared to free Ce6 treated MRSA. With the increased delivery efficiency and acceptable biocompatibility, the CS-Ce6 nanoassembly has a strong APDT effect on MRSA and *Acinetobacter baumannii* (*A. baumannii*) (Fig. 3e and f) [61]. Not only CS, its oligomers [70] and carboxymethyl CS (CMCS) [60] have also been shown as promising carriers for PSs. Mei et al. [70]

Table 1
List of polymer-PS's hybrid combinations fabricated for APDT.

Polymer	Type of PS	Bacterial pathogens	Excitation maximum	Concentration of PS	PDI efficiency	Ref
Maltoheptaose	BODIPY	*P. aeruginosa*	400–800 nm	800 μg/mL	90%	[32]
Bacterial EPS	RB	*E. coli* and *S. aureus*	532 nm	8 μM and 500 nM	100%	[55]
CMCS	Hp	*E. coli* and *S. aureus*	430–720 nm	15 μg/mL	97.19% and 98.38%	[60]
CS	Ce6	MRSA and *A. baumannii*	660 nm	4 and 40 μg mL^{-1}	100%	[61]
QAS-functionalized cellulose	PPIX	*drug-resistant S. aureus* and *E. coli*	white light	3.4 g L^{-1}	~100%	[62]
QAS-functionalized CS and HA	Ce6	*E. coli* and *S. aureus*	660 nm	120 and 20 μg/mL	~80%	[63]
Gelatin	*trans*-AB-porphyrin	*E. coli, Serratia marcescens, Pseudomonas putida, Bacillus subtilis* and *Candida viswanathii*	green LED light	4–8 μg/mL	~100%	[64]
CMCS	MBB	*S. aureus, E. coli, P. aeruginosa,* and MRSA	650 nm	2 μg/mL	100%, 95%, 97% and 99%	[66]
CS	Ce6	*E. coli* and *S. aureus*	660 nm	31.2 and 3.6 μg/mL	MIC	[69]
COS	GQDs	*E. coli* and *S. aureus*	450 nm	50 μg/mL	–	[70]
CS	ClAlPc	*S. mutans*	660 nm	8 μM	1 log_{10} CFU/mL	[76]
CS	Curcumin (CUR)	*S. aureus*	460–465 nm	25 μM	5.0 log	[89]
CS	sulfonated aluminum phthalocyanine	*S. aureus*	675 nm	5 wt%	20 ± 2 mm ZOI	[90]
PEG-*b*-PCL	HYP A	MRSA	470 nm	0.69 and 1.38 mg/L	MIC and minimum bactericidal concentration (MBC)	[57]
OC-conjugated PEI	Ce6	*E. coli and S. aureus*	630 nm	2.2 and 4.9 μg/mL	MIC	[67]
PPEGMA-*b*-P(DPA-*co*-TPPC6MA)	TPPC6MA	*S. aureus* and MDR *E. coli*	650 nm	–	–	[68]
PEI	PPIX	*E. coli, P. aeruginosa, S. aureus,* and *Staphylococcus epidermidis* (*S. epidermidis*)	635 nm	0.05 mg/mL for *S. epidermidis*, and 0.01 mg/mL for other bacteria	~100%	[74]
Chol-conjugated PEI	Ce6	*S. aureus* and *E. coli*	671 nm	2 and 10 μg mL^{-1}	100%	[75]
PEG-*b*-PCL and PCL-*b*-PAE	PPIX	*S. aureus* Xen36	630 ± 30 nm	80 μg mL^{-1}	100%	[78]
PAsp-*b*-PCL	PPIX	*S. aureus* Xen36	635 nm	200 μg/mL	100%	[79]
PNIPAM-*b*-PSt	Ce6	MRSA	White light	138 nM	6 log	[80]
Cationic PSeV	PSeV and UCNPs	MRSA	980 nm	2.5×10^{-6} M	98.3%	[84]
PVP	UCNPs and RB	XDR-AB	980 nm	50 μg/mL	4.72 log	[87]
Ethylenediamine-functionalized poly(glycidyl methacrylate)	Zinc(II) monoamino phthalocyanine	*E. coli* and *S. aureus*	700 ± 10 nm	128 μg mL^{-1} and 4 μg mL^{-1}	MBC	[91]
Pluronic® P123	HYP	*S. aureus*	orange LED	3.12 μmol/L	4.0 log	[92]
hyperbranched polyglycerol (hPG)	10,15,20-tris(3-hydroxyphenyl)-5-(2,3,4,5,6-pentafluorophenyl)porphyrin	*S. aureus*	652 nm	10 and 100 μM	100%	[93]
PEG-*b*-poly(2-(hexamethyleneimino) ethyl methacrylate-*co*-aminoethyl methacrylate)	Ce6	*S. aureus* and *E. coli*	660 nm	8 and 32 μg/mL	99.84% and 99.44%	[94]
oligo(*p*-phenylenevinylene) electrolytes	porphyrin–polyhedral oligomeric silsesquioxane conjugate	*E. coli* and *S. aureus*	400–700 nm	8 μM and 500 nM	>99.9%	[95]

synthesized a combinational therapeutic platform using CS oligosaccharide (COS)-functionalized graphene quantum dots (GQDs-COS) with significant photochemical transformation to induce ROS and heat when exposed to light. The glycosylation of PSs is expected to acquire stability as well as additional benefits such as cell-surface interactions and site-specific delivery. Water-soluble glycopolymers potentially increase the PDI efficacies of non-porphyrin PSs by promoting their bacterial adherence [32,71,72].

The host-guest interaction between PS-linked α-cyclodextrin (α-CD) and host molecules can integrate PS into the polymeric systems. PS-conjugated and nitric oxide (NO)-integrated pH-sensitive charge reversal supramolecular micelles were fabricated via host-guest interaction between poly(ethylene glycol)-$(KLAKLAK)_2$-2,3-dimethylmaleic anhydride (PEG-$(KLAKLAK)_2$-DA), Ce6-conjugated α-CD (α-CD-Ce6) and NO-conjugated α-CD. The as-prepared supramolecular micelles exhibited antifouling potential and prolonged circulation at pH 7.4. After treatment with drug-resistant bacterial biofilms, the supramolecular micelles exhibited stronger bactericidal ability under laser irradiation than in other treatments with or without irradiation. The bio experiments indicated that the pH-responsive NO release and APDT synergetic system caused minimum damage to healthy tissues while successfully destroying biofilm at low PS dosage and laser intensity [58]. Due to bacterial membranes' negative potentials, functionalizing polymer-PS hybrids with a cationic peptide may enhance adherence on the cell surface. As seen in Fig. 4a and b, the host-guest assembly of α-CD-Ce6 and PEG-*b*-polypeptide copolymer resulted in the formation of Pep@ce6 micelles. With the help of lasers, the ROS generated by Pep@Ce6 micelles could kill bacteria in localized wound infection (Fig. 4c) and eradicate biofilms via improving the membrane-penetration and targeted killing capacity (Fig. 4d and e) [59].

For APDT operations, several cationic polymers with stimuli-responsive or dual-mode treatment systems are available. Liu et al. [73] demonstrated a pH-sensitive theranostic poly(PEG methyl ether methacrylate)-*block*-[poly(2-(diisopropylamino) ethyl methacrylate-*co*-2-hydroxyethyl methacrylate)]-Ce6 (PPEGMA-*b*-P(DPA-*co*-HEMA)-Ce6) through the reversible addition−fragmentation chain transfer (RAFT) polymerization and post-modification process. The pH-sensitive P(DPA-*co*-HEMA) segment contributes to their specific bacterial targeting and cationic therapy under acidic conditions (pH

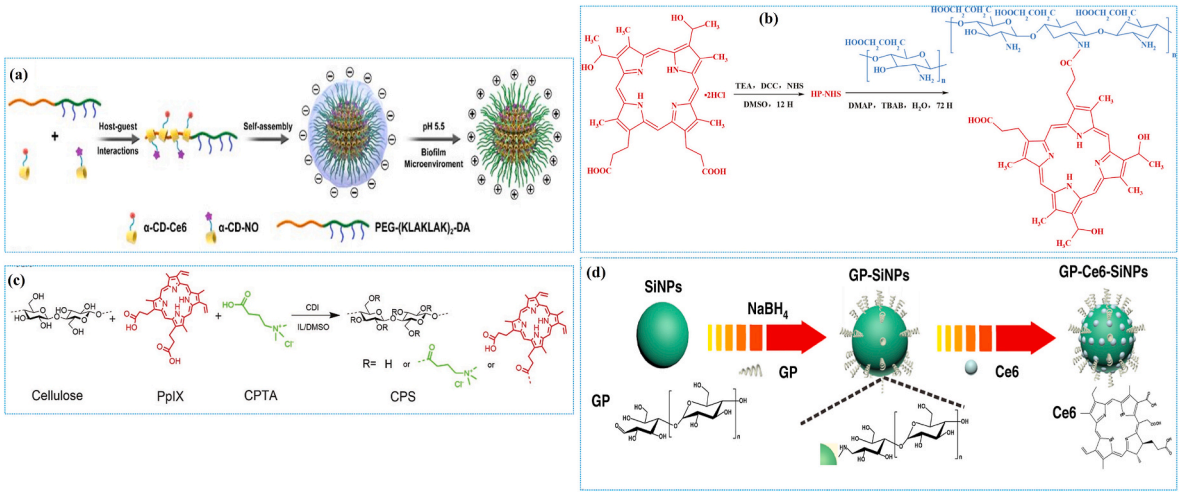

Fig. 2. Illustrations of the formation of polymer-PSs composites via different approaches: **(a)** Preparation of the PS-conjugated pH-responsive supramolecular micelles by host-guest interaction. Reprinted with permission from Ref. [58], Copyright © 2020, American Chemical Society. **(b)** CMCS-Hp composite conjugated via an amide linkage. Reprinted with permission from Ref. [60], Copyright © 2021, Elsevier. **(c)** Synthesis route of the PS-conjugated cellulose by covalent incorporation of PPIX and quaternary ammonium salt (QAS). Reprinted with permission from Ref. [62], Copyright © 2019, John Wiley and Sons. **(d)** Ce6-loading in poly [4-O-(α-D-glucopyranosyl)-D-glucopyranose-modified fluorescence silica NPs. Reprinted with permission from Ref. [65], Copyright © 2019, Springer Nature.

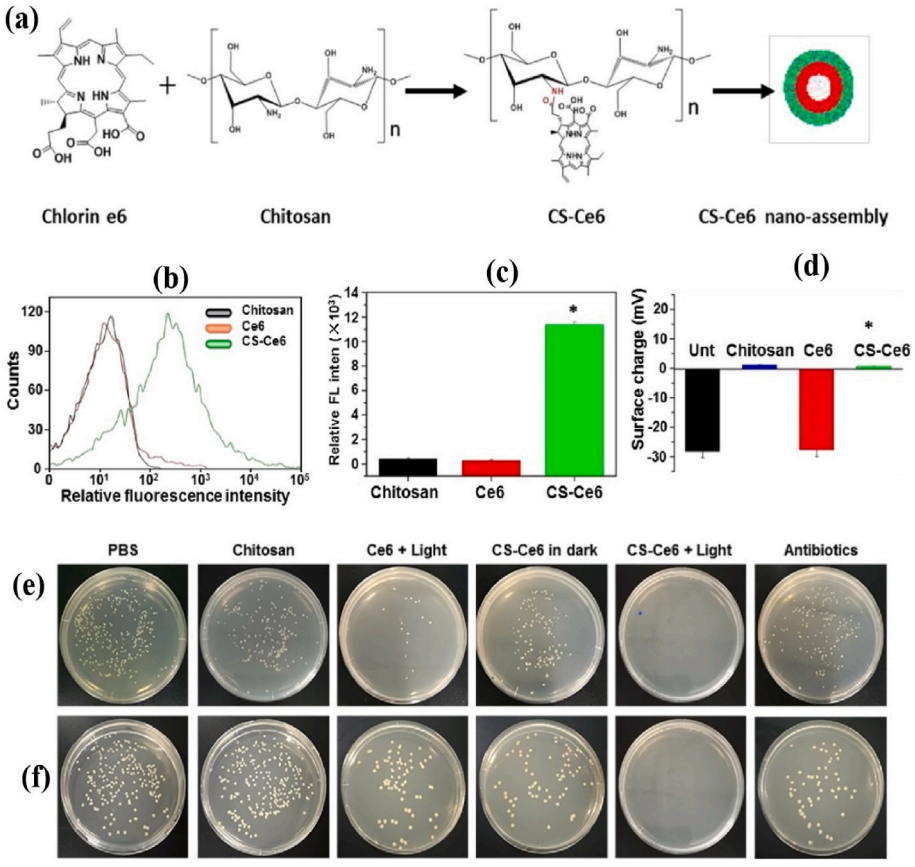

Fig. 3. **(a)** Schematic of the preparation of CS-Ce6 nanoassembly; **(b–d)** Flow-cytometry and zeta potential analysis of CS-Ce6 nanoassembly and MRSA mixtures; **(e–f)** *In vitro* APDT activity of Ce6 or CS-Ce6 nanoassembly against MRSA and *A. baumannii* with or without light irradiation. Reprinted with permission from Ref. [61], Copyright © 2019, American Chemical Society.

6.0). In another study, the acid-triggered porphyrin-based methacrylate (TPPC6MA) consisting of polymeric NPs (PPEGMA-*b*-P(DPA--*co*-TPPC6MA)) were fabricated via RAFT copolymerization. The as-assembled PPEGMA-*b*-P(DPA-*co*-TPPC6MA) NPs rapidly dissociate in the bacterial acidic condition (pH 5.5). This pH-responsive nature minimized the aggregation and raised a 5-fold $^1O_2$ yield with a high affinity to the negatively charged bacterial cell membrane surface [68].

The ROS-producing ability of PPIX in physiological media was improved by incorporating PEI. In the first trial, PPIX and PEI were mixed and treated under the hydrothermal condition, forming PPIX-PEI

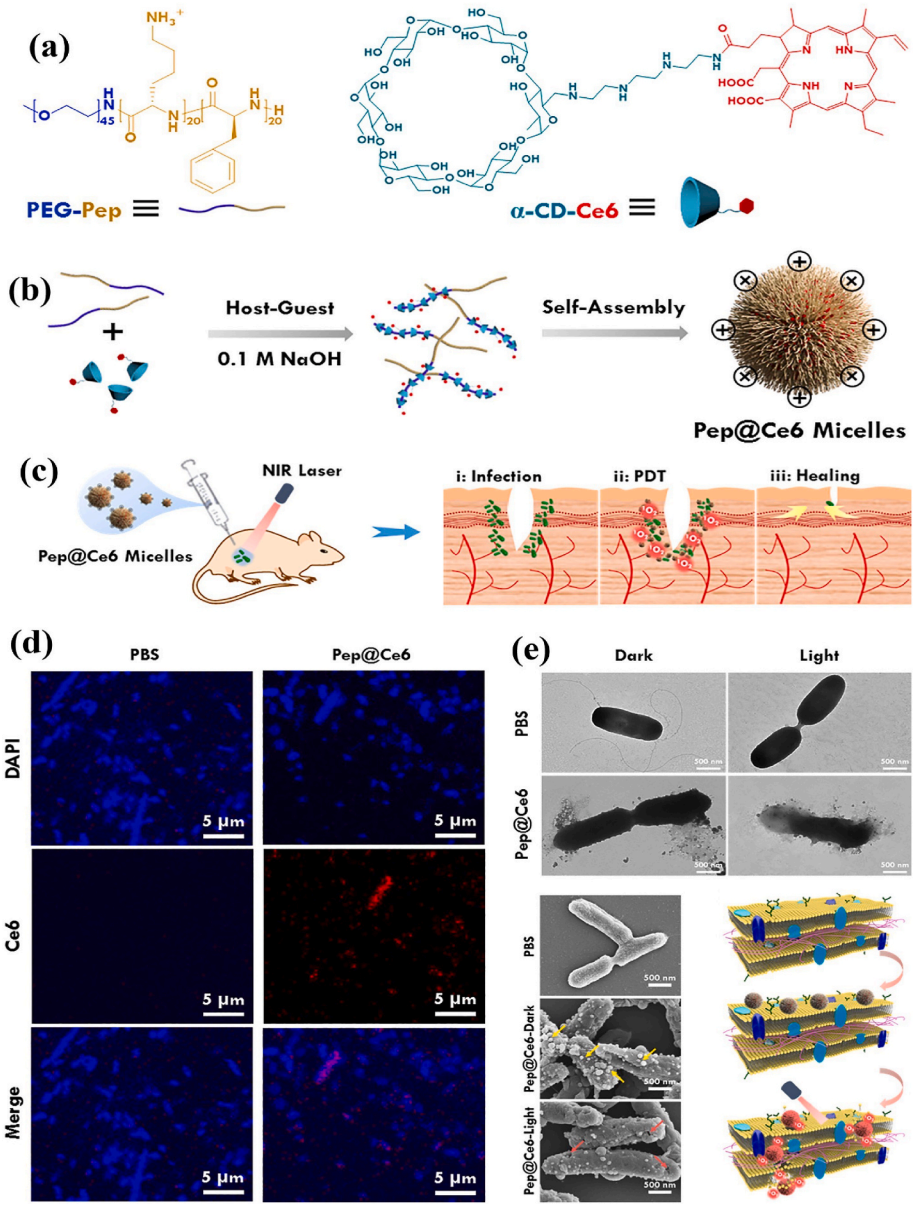

Fig. 4. (a–b) Schematic of the preparation of Pep@Ce6 micelles via host-guest interaction between PEG-*b*-polypeptide copolymer and α-CD-Ce6; **(c)** APDT action of Pep@Ce6 micelles against localized wound infections caused by *Pseudomonas aeruginosa* (*P. aeruginosa*); **(d)** Confocal laser scanning microscopy (CLSM), and **(e)** transmission electron microscopy (TEM) and scanning electron microscopy (SEM) images of *P. aeruginosa* treated with phosphate buffered saline (PBS) and Pep@Ce6 micelles with/without light irradiation. Reprinted with permission [59], Copyright © 2021, Elsevier.

NPs. However, the as-prepared PPIX-PEI-NPs demonstrated only negligible APDT effect on Gram-negative bacteria mainly because of their structural barrier to ROS [74]. Diverse classic membrane anchoring lipid molecules, such as cholesterol (Chol), phospholipids, and fatty acids, can be incorporated to facilitate engineering materials' cell surface binding ability. The highly water-soluble PEI was conjugated with hydrophobic Chol to form the lipopolymer micelles, which made conjugation of Ce6 (Chol-PEI-Ce6) easy through the formation of amide bonds. Under light irradiation, the Chol-PEI-Ce6 promoted the damage of bacterial cell membranes and leakage of intracellular contents in both *S. aureus* and *E. coli*. The increased bacterial-killing efficiency of Chol-PEI-Ce6 denotes the significance of Chol and low-molecular-weight PEI in polymer-based APDT strategies [75].

3.2. Polymer/photosensitizers-engineered nanomaterials

Engineering of nanostructured polymer-based materials bestows combinational phototherapeutic effects. PSs can be either blended with a polymeric reaction mixture or become physically entrapped inside the matrices to form the PS-loaded polymeric NPs. The CMCS-methylbenzene blue (MBB) NPs were successfully produced via the electrostatic interactions between CMCS and ammonium MBB. The as-synthesized CMCS-MBB NPs showed the pH-responsive sustained release of MBB and presented effective antibacterial activity against *E. coli*, *P. aeruginosa*, MRSA and *S. aureus* after 650 nm laser irradiation at 202 mW cm^{-2} for 5 min [66]. The ionic gelation process was adopted to encapsulate with chloroaluminium phthalocyanine (ClAlPc) in CS NPs, which exhibited a significant PDI effect on *Streptococcus mutans* (*S. mutans*) biofilm compared to free ClAlPc [76]. Moreover, the Ce6-loaded amphiphilic octanoyl chloride (OC)-functionalized PEI (OC-PEI) polymeric micelle also showed improved PDI action compared to free Ce6 [77].

Encapsulating hypocrellin (HYP) in the lipase-sensitive methoxy PEG-*block*-PCL (mPEG-*b*-PCL) micelles enhanced its biocompatibility, solubility, and target specificity. Furthermore, the PCL segment was biodegraded to release HYP after the micelles interacted with lipase-producing bacteria [53]. Interestingly, the PPIX-loaded mixed shell polymeric micelles (MSPMs) comprised of PEG-*b*-PCL and PCL-*block*-poly(*β*-amino ester) (PCL-*b*-PAE) presented pH-dependent charge reversal properties to target bloodstream biofilm. Furthermore, the PPIX-loaded

MSPMs produced ROS in the vicinity of the concerned pathogens under light irradiation, which resulted in enhanced APDT than the PPIX-loaded polymeric micelles consisting solely of PEG-*b*-PCL [78]. Compared to polymeric micelles-based monotherapy, the combination of silver nanoparticles (AgNPs) and PPIX enabled the resulting polymeric composite to exert chemo-PDT against MDR bacterial pathogen (*S. aureus* Xen36). Furthermore, the prepared polymeric composite exhibited robust bactericidal efficacy against subcutaneous infections induced by *S. aureus* Xen36 in a murine model [79].

Polymer functionalized NMs such as silica NPs [65], metals [80,81], metal oxides [82], carbon dots [83], graphene oxide (GO) [56], upconversion NPs (UCNPs) [84] and graphite-like carbon nitride (g-C_3N_4) nanosheets (NSs) [85] were explored for APDT applications either solely or in combination with other PSs. Ce6-loaded and poly [4-O-(α-D-glucopyranosyl)-D-glucopyranose-modified fluorescence silica NPs unveiled a better PDI effect against *S. aureus* (98%) and *P. aeruginosa* (96%), which can be potentially exploited as imaging and APDT platform [65]. The AgNPs-stabilized and Hp-loaded poly(*N*-isopropylacrylamide)-*block*-PSt (PNIPAM-*b*-PSt) NMs demonstrated enhanced $^1O_2$ generation efficiency, and high PDI against both *S. aureus* and *E. coli*, in comparison to the free Hp molecule [81]. Wang et al. [86] modified the Ce6-loaded manganese dioxide NPs (MnO_2 NPs) with PEG, leading to the formation of Ce6@MnO_2-PEG NPs. The MnO_2 NPs could convert H_2O_2 into O_2 to improve the microenvironment of the abscess. Compared to free Ce6, the Ce6@MnO_2-PEG NPs revealed better APDT efficacy in oxygen-deficient and H_2O_2-enriched environments. It was also noticed that the Ce6@MnO_2-PEG NPs triggers immunological memory responses by releasing adjuvant-like manganese ions to prevent abscess relapses resulting from the same type of bacterial infection (Fig. 5a–c).

Some nanostructured materials can be used as platforms to support the PSs and enhance the quality of treatment. Recently, the functionalization of zinc phthalocyanine with low-molecular-weight triethylene glycol monomethyl ether (TEGMME) significantly increased the solubility and biocompatibility of resulting phthalocyanine-TEGMME@GO composites. Although the phthalocyanine-TEGMME conjugates exhibited higher $^1O_2$ yields than the phthalocyanine-TEGMME@GO composites, GO's plausible photothermal conversion efficiency offers synergistic bactericidal and speeded up wound repair activities [56]. Upon 980 nm laser irradiation, the poly(selenoviologen) (PSeV)-functionalized UCNPs (UCNPs/PSeV) hybrids could efficiently generate more ROS than common PSs (methylene blue (MB) and RB). The as-synthesized UCNPs/PSeV could yield an efficient synergistic APDT and APTT to kill MRSA in deep tissue [84]. The light adsorption and ROS generating rate of RB were improved at NIR biological windows (700–1000 nm) after loading with polyvinylpyrrolidone (PVP)-UCNPs (LiYF4: Yb/Er). Moreover, the UCNPs-PVP-RB nanosystem remarkably inhibited the growth of drug-resistant *A. baumannii* (XDR-AB) in a dose-dependent manner. Microscopic examinations (TEM and SEM) disclosed that the surface of XDR-AB was disrupted immediately after APDT and resulted in excessive membrane permeability and protein leakage (Fig. 5d–g) [87].

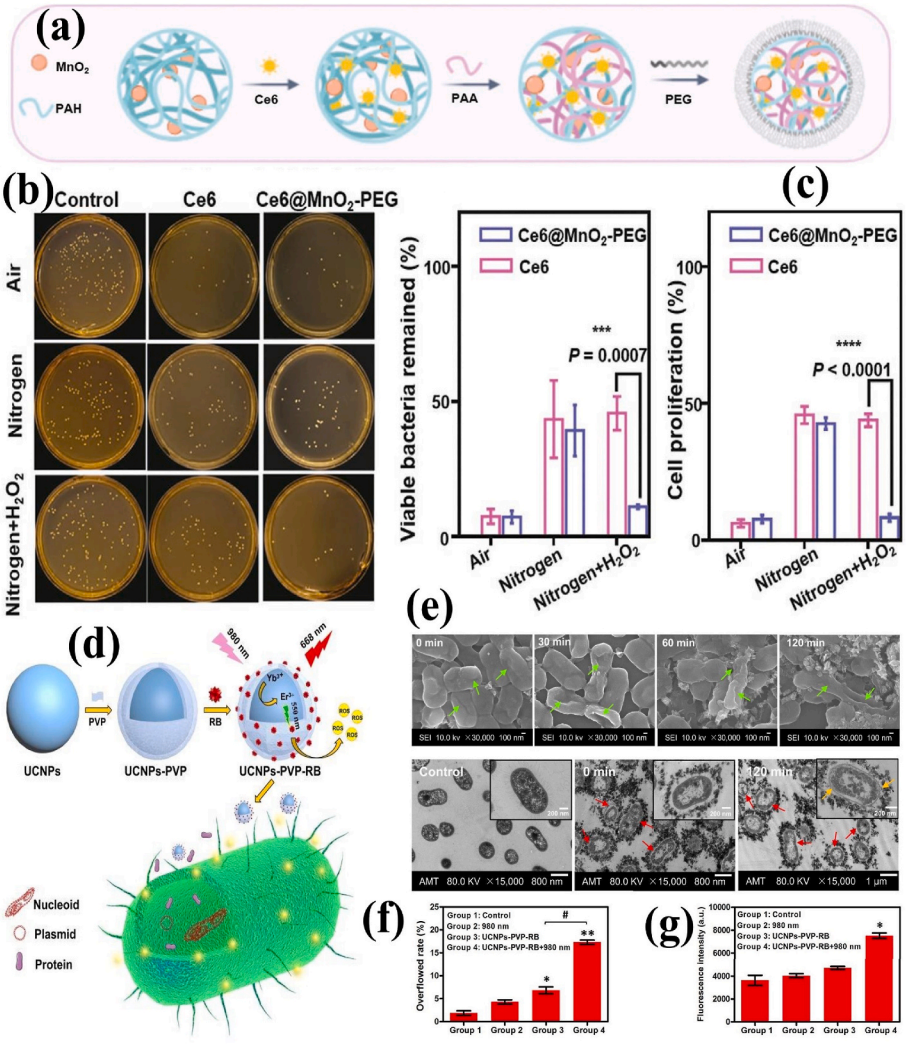

Fig. 5. **(a)** Schematic of the synthesis of Ce6@MnO_2-PEG NPs; **(b)**Viable bacteria remained in the culture after APDT treatments; **(c)** Cell proliferation of *S. aureus* measured by 3-[4,5-dimethylthiazol-2-yl]-2,5 diphenyl tetrazolium bromide (MTT) assay after treatments. Reprinted with permission [86], Copyright © 2020, John Wiley and Sons. **(d)** Schematic of UCNPs-PVP-RB synthesis and its APDT action; **(e)** SEM (top) and TEM (bottom) images of XDR-AB after APDT (0–120 min); **(f)** Cell membrane permeability; **(g)** Cell membrane integrity of XDR-AB after APDT. Reprinted with permission from Ref. [87], Copyright © 2020, Royal Society of Chemistry.

Nevertheless, the limited $^1O_2$ generation in hypoxic microenvironments, less effectiveness against deep tissue bacteria and inflammation must be resolved for clinical translation. In a recent report, multifunctional PEGylated partially oxidized tin disulfide (SnS_2) NSs (POS NSs) and UCNPs composite loaded with ICG molecules (POS-UCNPs/ICG) showed the potential to generate O_2 and CO therapeutic gases upon 808 nm NIR irradiation. The up-conversion of deep tissue penetrating NIR into visible green light activates the photocatalysis of POS NSs to produce CO and O_2 gases, and APDT action of ICG molecule. The bacterial survival rate of *S. aureus* and *E. coli* decreased to zero with 50 μg mL^{-1} POS-UCNPs/ICG treatment. However, the therapeutic effect of *S. aureus* is better than that of *E. coli* due to the blockage of ROS attack by cell membrane lipopolysaccharide. The CO molecule formed by POS-UCNPs/ICG nanoplatform have shown the ability to modulate macrophage polarization via the phosphoinositide 3-kinase (PI3K)-mediated NF-κB pathway and trigger anti-inflammatory effects (Fig. 6a–d) [88]. The engineered polymer-PS hybrid composites could collectively provide novel strategies to improve the APDT performances of PSs with excellent biocompatibility. In addition, the enhancement of $^1O_2$ generation favors lower cytotoxicity and excludes MDR formation. The above information recommends that the NMs/polymer/PSs hybrid integrations offer beneficial platforms for eradicating site-specific and deep-tissue infections without non-specific side effects.

4. Surface coatings

Implant-associated infections (IAIs) have become a significant burden on healthcare systems and caused huge economic losses at the societal level. Under appropriate circumstances, communities of bacterial pathogens can hold together and form complex biofilms on the surface of biomaterials. These biofilms can produce EC polymeric substances, such as proteins, polysaccharides, and lipids, to give rise to antibiotic resistance [96,97]. Long-term exposure to antibiotics and other sterilization methods has complicated biofilm eradication because of antibiotic depletion, the emergence of MDR bacteria, and other undesirable side effects. Also, the infections caused by pathogens during the lifetimes of implants inevitably result in their failure [13]. APDT is an instantaneous option with controlled and high spatiotemporal precision for medical devices [98,99]. Hence, the construction of the APDT coatings with high ROS yields facilitates protection against IAIs.

Various surface coating technology enriched with functional materials has been developed to resist the IAI's in orthopedic implants [100–102]. Polydopamine (PDA) is a crucial mussel-inspired biopolymer well known for its unique properties like universal adhesion and rapid deposition on implant surfaces [103–105]. Furthermore, the PDA coating dramatically increased photon-absorption capacity, biocompatibility, and surface post-functionalization capability [106]. Multifunctional PDA-based coating technology has been developed in biocompatible orthopedic substrates. The deposition of Ag_3PO_4-GO composites onto the PDA-treated medical-grade titanium (Ti) plates or polyetheretherketone (PEEK) sheets bestowed synergistic bacterial killing surfaces. By varying the amount of GO in the hybrid coatings, the bandgaps of the Ag_3PO_4 NPs can be tuned from 2.52 to 2.0 eV. Upon irradiation with 660 nm visible light, the hybrid PDA/Ag_3PO_4/GO coatings retained consistent antibacterial efficacy via releasing Ag^+ ions and ROS (Fig. 7a) [107]. Loading AgNPs onto GO NSs and wrapping the composites with a thin layer of Type I collagen increased ROS level under visible light irradiation. The engineered-implant surfaces could

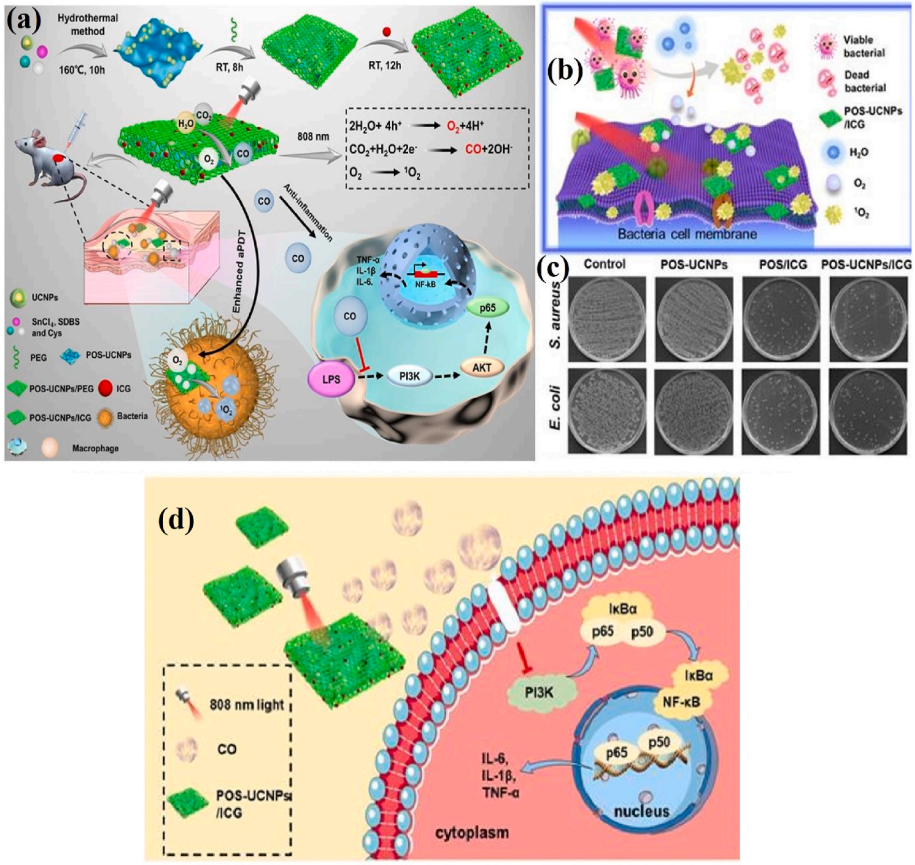

Fig. 6. **(a)** Schematic of the preparation of POS-UCNPs/ICG composite and its APDT mechanism; **(b)** Schematic of POS-UCNPs/ICG induced bacterial damage; **(c)** Bacterial colonies after treatment with different concentrations of prepared composite; **(d)** Schematic of POS-UCNPs/ICG triggered anti-inflammation mechanism via CO production. Reprinted with permission [88], Copyright © 2022 Ivyspring International Publisher.

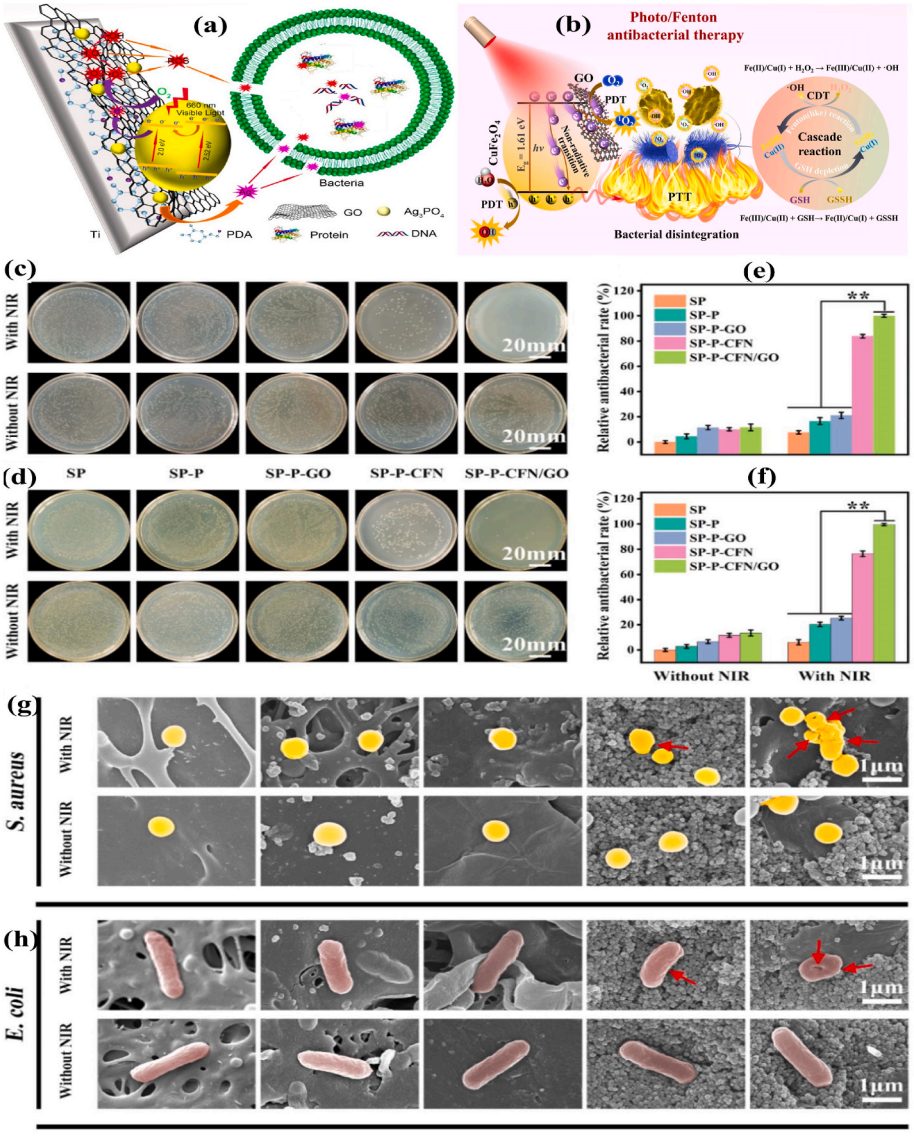

Fig. 7. (a) Schematic of hybrid PDA/Ag_3PO_4/GO-based antibacterial coating on Ti implant. Reprinted with permission [107], Copyright © 2018, American Chemical Society. **(b)** Schematic of NIR-triggered synergistic antibacterial mechanism of $CuFe_2O_4$/GO; **(c–d)** Photographs of *S. aureus* and *E. coli* bacterial colonies treated by different samples with/without NIR irradiation; **(e–f)** The relative antibacterial percentages of *S. aureus* and *E. coli*; **(g–h)** SEM morphologies of bacteria treated with different samples (the red arrows indicate the membrane shrinkages). Reprinted with permission [110], Copyright © 2021, Elsevier.

achieve high antibacterial efficacy of 96.3% and 99.4% against *E. coli* and *S. aureus*, respectively, with 660 nm light in subcutaneous tests [108].

By combining APTT and APDT formulations, the NIR-absorbing materials raise the local temperature, making the bacterial membranes more sensitive to ROS. Furthermore, the oxidation of glutathione (GSH) to glutathione disulfide is considerably enhanced by hyperthermia, resulting in a depletion of the bacterial antioxidant system and improved lethality of bacterial cells. Wang et al. [109] assembled GO NSs, PDA, and bone-forming peptide (BFP, in a sequence of GQGFSYPYKAVFSTQ) onto the surface of porous sulfonated PEEK. The GO-PDA-BFP-decorated PEEK surfaces exhibited synergetic APDT and APTT therapeutic effects due to the π-π stacking interactions between PDA and GO. In a recent study, the heterojunction coating of GO hybridized with copper ferrite ($CuFe_2O_4$) was deposited on a PDA-deposited sulfonated PEEK implant. A decrease in the emission intensity of $CuFe_2O_4$/GO-functionalized sulfonated PEEK (SP-P-CFN/GO) compared with GO-functionalized sulfonated PEEK (SP–P-GO) at 345 nm indicates the rapid electron transfer from $CuFe_2O_4$ to GO and substantial improvement of $CuFe_2O_4$/GO photocatalytic performance. Also, the reduced bandgap width of $CuFe_2O_4$ (1.72 eV) than $CuFe_2O_4$/GO (1.61 eV) manifests that the conductive heterojunction coating favors electron escape and stimulates ROS production. Exposure to heterojunction coating in a slightly acidic environment raises the emancipation of elements (Cu, Fe), which depicts the boosted nutritional element discharge in the bacterial pathogenic milieu. As a result, the osteogenesis and osseointegration between the implant and bone tissue have been strengthened through photo-triggered therapeutic ions delivery (Fig. 7b–h) [110].

The mesoporous PDA NPs were deposited on the Ti substrates, followed by the immobilization of osteogenic peptide arginine-glycine-aspartic acid (RGD) and loading of ICG. Through the combined effects of hyperthermia and ROS under dual-wavelength light (660 nm + 808 nm) irradiation, the RGD-ICG-PDA-modified surfaces demonstrated impressive osteoconductivity and biofilm eradication capacities [111]. In another study, the triple therapeutic platform of biocompatible PDA-ICG-daptomycin coating was deposited on the Ti implants. The release of daptomycin inhibited the growth of *S. aureus*. After 808 nm laser irradiation, the collective effort of hyperthermia and $^1O_2$ eradicated the biofilm noninvasively [91]. The CS@molybdenum disulfide (MoS_2) nanocomposites were coated onto the modified Ti implants via the electrophoretic deposition technique. Despite their effective NIR (808 nm) absorption due to MoS_2 incorporation, only a moderate APTT effect (64.67% and 57.44%, respectively) was recorded, while the visible light treatment induced a high APDT effect (91.58% and 92.52%, respectively) on *E. coli* and *S. aureus*. Hence, the dual irradiation (NIR & visible light) of CS@MoS_2 promotes the photo-killing efficiency of up to

99.84% and 99.65% against *E. coli* and *S. aureus*, which can be endorsed by the combined effects of heat and ROS [112].

A few PSs-PDA-hydrogel-based coating technologies with multiple functions have been established for better regenerative applications. The catechol motif-modified methacrylated gelatin and Ce6-loaded mesoporous PDA NPs hydrogel has shown a great affinity toward Ti surfaces, and possesses both antibacterial activity and fibroblast activation ability [113]. Likewise, the deposition of CS, PDA, and a NO release donor (RSNO)-containing viscous poly(vinyl alcohol) (PVA) hydrogel on red phosphorus (RP) nanofilm-coated Ti implant (Ti-RP/PCP/RSNO) effectively destroys bacterial biofilm (Fig. 8a). As shown in Fig. 8b–d, the Ti-RP/PCP/RSNO coating renders peroxynitrite ($ONOO^-$), a byproduct of the reaction between NO and $^{\bullet}O_2^-$. The synergistic action of $ONOO^-$ and hyperthermia drastically decreases ATP activity and causes bicinchoninic acid leakage from MRSA. Under NIR irradiation, the released NO up-regulates the osteogenic genes, Ca^{2+} deposition, and M1 polarization of macrophages, unveiling that the MRSA-infected tissues could be repaired without surgery using photo-immunotherapy [114]. The surface engineering of biomedical materials and devices benefited from the flexibility, tear/abrasion resistance, tensile strength, and thermal stability of polymer-PSs coatings. In addition, the co-integration of photo absorbing NMs and PSs in the coatings improves the vulnerability of bacteria to hyperthermia due to additional oxidative lesions. The diffused ROS from the PSs-embedded biomedical surface increases planktonic bacterial membrane porosity and cytoplasmic membrane damage, and biochemical alterations. Improved superhydrophobicity of PSs surfaces have been designed to reduce/inhibit bacterial adherence, colonization, and biofilm formation.

5. Films, scaffolds and hydrogels

5.1. Photosensitizers-incorporated films and scaffolds

Extensive studies have been conducted to generate self-disinfecting antibacterial polymeric biomaterials by integrating PSs via dip-coating, swell-encapsulation-shrink, surface adsorption, chemical conjugation, and physical mixing for APDT applications [90,115]. Polyurethane (PU) and polydimethylsiloxane (PDMS) are important polymeric substrates for preparing biomedical implants and devices. As a result, many research works have been undertaken to develop photoactive PU and PDMS with different combinations of PSs for restricting IAIs [116–121]. Noimark et al. [122] prepared a medical-grade PDMS incorporated with crystal violet (CV) and zinc oxide (ZnO) NPs using a simple swelling strategy. The results suggest that the CV-ZnO-embedded

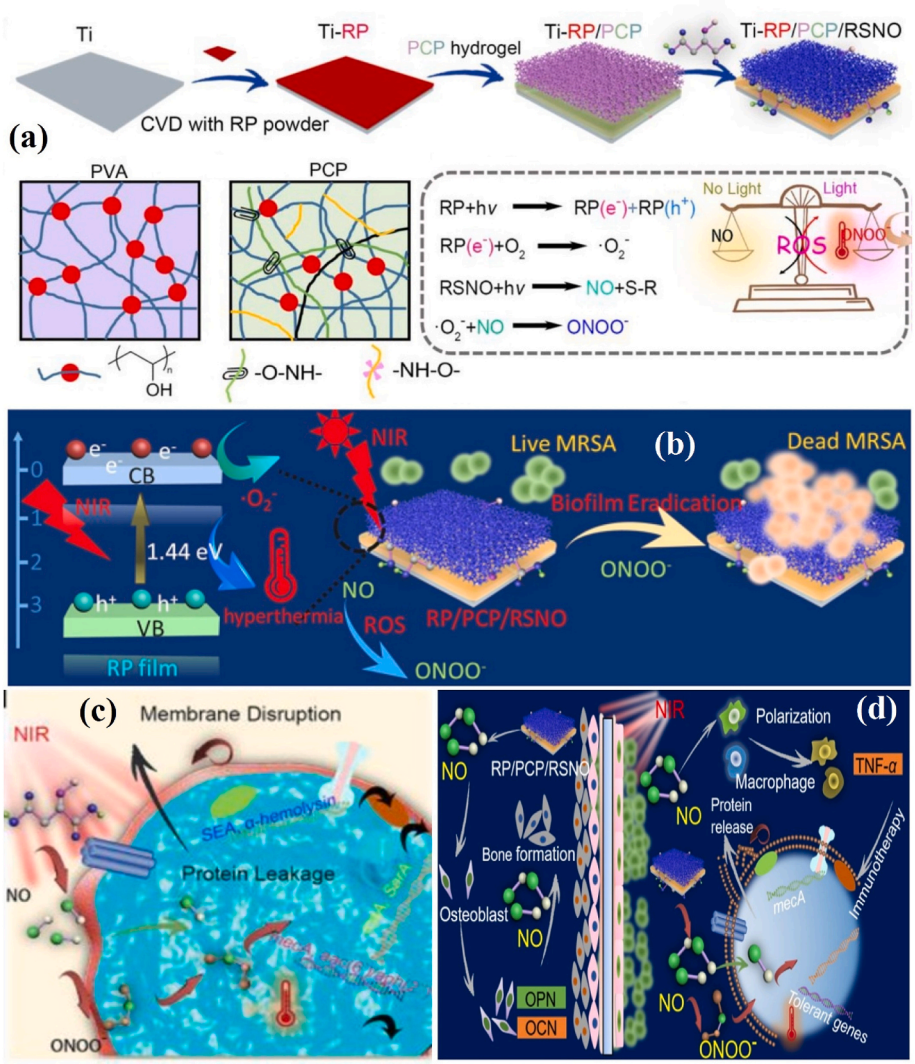

Fig. 8. **(a)** Schematic of the preparation of RSNO-loaded PCP hydrogel coating and its photochemical mechanism; **(b)** Schematic of NIR-induced MRSA biofilm elimination; **(c)** Schematic of bicinchoninic acid leakage from MRSA after NIR irradiation; **(d)** Schematic of bone regeneration through M1 polarization of macrophages and MRSA biofilm eradication through gene downregulation. Reprinted with permission [114], Copyright © 2020, American Chemical Society.

PDMS substrate exhibited a higher visible light-induced APDT effect than the silver- and nitrogen-doped thin films. The carbon QDs (CQDs)-based PSs with zero dimension and below 10 nm size range were incorporated on PU surfaces to combat various bacterial pathogens using different irradiation sources. The diffused ROS from the CQDs-embedded PU surface increases bacterial membrane porosity and causes cytoplasmic membrane damage and lipid peroxidation [123]. Using a similar technique, a functional PU deposited was reported with a combination of indium-based cadmium-free QDs and CV. This study deliberated that the photo-physical interactions of indium-based QDs with CV activate Type I and Type II electron and energy transfer processes. The indium-based QDs- and CV-embedded PU surface exhibits synergistic killing effects on the clinical and environmental strains under low power visible light illumination [124]. The deposition of natural HYP with (2-hydroxypropyl)-β-CD inclusion complex (HYP-β-CD) can also be used in PU-based biomedical implants safely and effectively to overcome catheter-related bloodstream infections [125]. The superhydrophobic polylactic acid (PLA) surface was achieved via a facile non-solvent-assisted induced phase separation process, followed by surface adsorption of natural Chl. The incorporation of Chl does not influence the superhydrophobicity of PLA. The synergistic antibacterial PLA surface and mask exhibit tremendous antibacterial efficiency against *S. aureus* and *E. coli*, because of their superhydrophobicity and APDT performance under visible light illumination [126].

Electrospinning is a facile and cost-effective technique to efficiently produce PSs combined fibrous micro/nano architectures with a maximum production rate. Compared with other spinning techniques, the PSs-loaded fibrous scaffolds fabricated by electrospinning are smaller with improved photobactericidal properties [127]. Further, the immobilization of PSs on electrospun scaffolds via covalent attachment is more robust than non-covalent interactions and endows the fibrous surfaces with increased $^1O_2$ diffusion. The improved physical characteristics like large surface area, stability, surface area to volume ratio, and porosity make PSs integrated scaffolds prominent in many regenerative medicine applications.

The mixture of sulfonated aluminum phthalocyanines and CS were electrospun into nanofibrous mats. Based on the findings, it can be concluded that the uniformly dispersed PS-CS fibers exhibit remarkably strong light-induced antibacterial activity against *S. aureus* [90]. PPIX-embedded cellulose diacetate (CA) microfibers membrane displays an improved $^1O_2$ generation under Xe lamp illumination (65 $\pm$ 5 mW/cm^2, $\lambda \geq$ 420 nm, 30 min). In this formulation, the potassium iodide actively potentiated its bactericidal efficiency (6 log units) via forming alternative microbicidal species, i.e. combination of I_2, I_3^-, I· and $I_2{\cdot}^-$ (Fig. 9a) [128]. An advanced sulfonated electrospun PSt nanofiber membrane was fabricated with biotin molecules via a "click" reaction. This biotinylated fibrous membrane was ionically bonded with cationic 5,10,15,20-testrakis(1-methylpyridinium-4-yl)porphyrin tetra (*p*-toluenesulfonate) (TMPyP). Furthermore, horseradish peroxidase and streptavidin conjugation preserve the resulting multifunctional membranes' enzymatic activity and PDI effect (Fig. 9b) [129]. Another study proved that exchangeable cations in composite nanofibers could absorb more MB and inactivates bacterial pathogens under photonic irradiation [130]. In contrast, certain fabrics loaded with tetra-anionic 5,10,15,20-tetrakis(4-sulfonatophenyl)-21H,23H-porphine (TPPS) (Fig. 9c) was not effective against Gram-negative strains due their inherent tolerance [131]. Likewise, the immobilization of other PSs such as PPIX and HYP onto BC showed a PDI effect only against either Gram-positive or Gram-negative pathogens, respectively [132]. Considering this, the polyanionic poly(γ-glutamic acid) (γ-PGA) and cationic TMPyP fibrous mats cross-linked with 1,2-bis(2-aminoethoxy) ethane were fabricated as the effective APDT platform against both Gram-positive and Gram-negative pathogens [133]. The above literature shows that the engineered-nanofibrous materials of zwitterionic nature might deliver an effective photobactericidal effect.

However, most fibrous scaffolds were constrained with burst release,

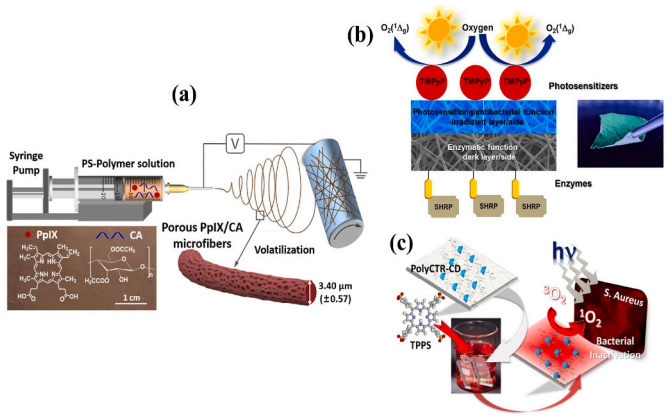

Fig. 9. **(a)** Preparation of the porous PPIX/CA membrane by electrospinning. Reprinted with permission [128], Copyright © 2021, Elsevier. **(b)** Schematic of the PS- and enzyme-decorated multifunctional nanofiber composite. Reprinted with permission [129], Copyright © 2020, American Chemical Society. **(c)** Preparation of the CD-functionalized and TPPS-loaded PP fabric and its APDT mechanism. Reprinted with permission [131], Copyright © 2017, American Chemical Society.

which had undesirable side effects. Therefore, constructing electrospun membranes with on-demand delivery nanoplatforms is highly anticipated [134]. To address this, Zhang et al. [135] recently prepared a zeolitic imidazolate framework-8/PLA (ZIF-8/PLA) electrospun fibrous membrane loaded with CUR-ICG (CUR-ICG@ZIF-8/PLA, CIZP) and coated with phase-change material (CIZPP, Fig. 10a–c). The SEM micrographs showed the uniform distribution of CUR-ICG@ZIF-8 nanocrystals on PLA fibers with increasing diameter from 0.85 $\pm$ 0.2 μm to 1.10 $\pm$ 0.30 μm upon modification with phase-change material (Fig. 10d and e). The "on-off" NIR irradiation stimulates the release of CUR mainly because of the thermo-responsive solid-liquid transition of phase-change material and ZIF-8 degradation in the acidic microenvironment (Fig. 10f and g). Further experimental evidence shows CIZPP might prevent MDR bacterial infection via causing cell membrane damage.

Other PSs-containing multifunctional fibers and scaffolds have been prepared for hemostasis, bacterial elimination, wound monitoring and repair [136]. Overall, the PSs encrusted scaffolds offer a cutting-edge approach for engineering biomaterials with APDT platforms in tissue/-bone regeneration and wound repair applications.

5.2. Photosensitizers-incorporated hydrogels

Bacterial infections became a severe problem in wound treatment due to tissue damage and a slow healing process. Hence, the need for advanced wound care products is rising in the global wound care market [137]. In particular, polymer-based hydrogels mimicking EC matrix have received increasing attention due to their stupendous swelling behavior and ability to provide a moist environment on the wound site. However, the hydrogel precursors often showed good biocompatibility and negligible bactericidal effect. Therefore, the PS-loaded hydrogels were developed for photo-induced ROS production and bactericidal action in wound-care applications [138,139].

Inorganic NMs were primarily used in multifunctional hydrogel preparation. For instance, the negatively charged black phosphorus (BP) was embedded in positively charged CS hydrogel (CS-BP) through electrostatic attraction. As shown by the results of this study, the bacteria-killing efficiency of CS-BP hydrogel was increased up to 99% under simulated sunlight irradiation for 10 min. Interestingly, the CS-BP treatments triggered the signaling pathways of PI3K, phosphorylation of protein kinase B (Akt), and EC signal-regulated kinase (ERK1/2), which induced rapid cell proliferation, differentiation, and EC matrix synthesis in skin regeneration (Fig. 11a) [140].

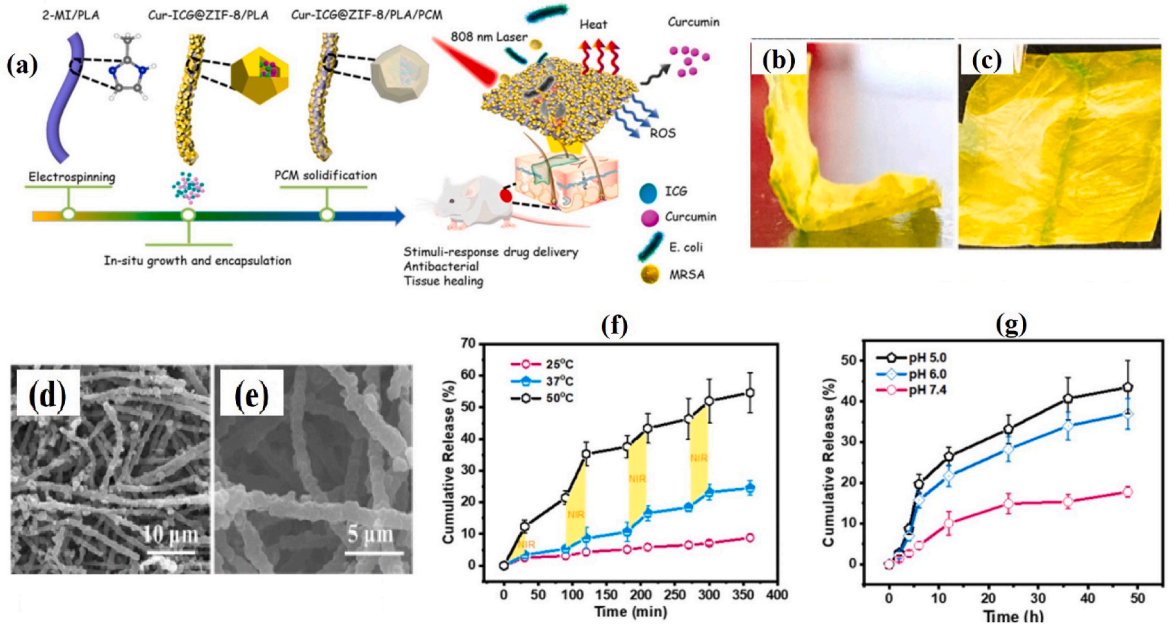

Fig. 10. **(a)** Schematic of CIZPP synthesis and its application; **(b and c)** Photographs of as-prepared CIZPP electrospun membrane; **(d and e)** SEM micrographs of CIZPP fibers; **(f)** NIR- and (b) pH-triggered CUR release profile from CIZPP electrospun membrane. Reprinted with permission [135], Copyright © 2022, Elsevier.

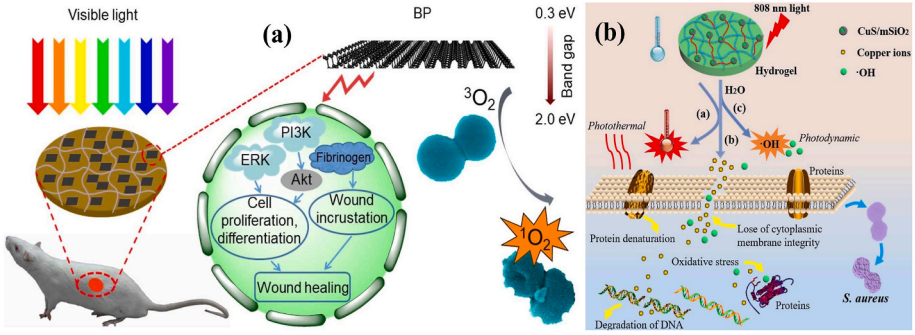

Fig. 11. **(a)** Schematic of preparation of the CS-BP hydrogel as well as its antibacterial PDI and wound healing mechanisms. Reprinted with permission [140], Copyright © 2018, American Chemical Society. **(b)** Schematic of the bacteria killing processes with the hybrid CuS-embedded thermo-responsive hydrogel under 808 nm NIR irradiation. Reprinted with permission [142], Copyright © 2018, Royal Society of Chemistry.

To enhance the APDT effect of PSs-incorporated hydrogels, several PSs and photothermal agents combined hydrogels have been prepared recently [141]. Since RB cannot be directly loaded into the hydrogel due to its water solubility, it was covalently grafted onto the CS microspheres. The aldehyde-functionalized β-CD was conjugated with amine-containing GO, leading to the formation of β-CD-modified GO. The RB-loaded CS microspheres, β-CD-modified GO, and PVA were mixed to form the hybrid hydrogel via the freezing and thawing method. In preclinical studies, the GO-induced hyperthermia combined with RB-generated ROS under 808 and 550 nm light irradiation gave excellent antibacterial activity [57]. The hydrophilic polymer-based hydrogel mechanically supported with copper sulfide (CuS) NPs gives high moisture conditions, facilitating the proliferation of viable cells and releasing growth factors. The CuS-based NPs have been proposed as both PSs and photothermal agents in antibacterial therapy. In a lower critical solution temperature (LCST), the NIPAM and acrylamide segments underwent changes in volume conformation according to minor temperature variations, and the volume change caused by hyperthermia under NIR light irradiation could regulate the release rate of Cu ions (Fig. 11b) [142]. Another study demonstrated that the lignin-CuS nanocomposites incorporated PVA hydrogel exhibit peroxidase-like performance and phototherapeutic actions [143]. In some formulations, the photothermal agents act as carriers and protect PSs excretion, ultimately enabling rapid wound closure via protecting endothelial and promoting neovascularization [144].

The sinoporphyrin sodium (DVDMS) essential fibroblast growth factor (bFGF)-loaded poly(lactic-*co*-glycolic acid) were embedded into the CMCS and sodium alginate hydrogels. Under mild photoirradiation (30 J/cm^2, 5 min), the multifunctional hydrogel inactivated almost 99.99% of *S. aureus* and MDR *S. aureus*. In the burn-infection model, the multifunctional hydrogels inhibit bacterial growth and promote wound healing [145]. Recently, the integration of antimicrobial peptide (*ε*-poly-L-lysine) in *g*-C_3N_4-based hydrogel with APDT effect contributes to sustained antibiosis and immunomodulation, as well as regulates inflammation in cutaneous wound [146]. In addition, the bioactive CMCS and sodium alginate hydrogel assimilated with berberine (a quorum sensing (QS) inhibitor and antibacterial agent)-loaded natural living microalgae *Spirulina platensis* could accelerate MRSA-infected diabetic wound healing by promoting angiogenesis and skin regeneration, and suppressing the inflammatory response [147]. All these efficient combination strategies with multiple functions can be effectively used to treat non-healing wounds.

5.2.1. Injectable hydrogels

Skin wounds are often irregular in form, posing a challenge for traditional hydrogels as they cannot cover most wound areas. Also, the implantation of pre-formed hydrogels on irregular wounds requires a high-cost invasive surgical procedure that can cause patient discomfort and inflammation [148,149]. As an alternative to pre-formed hydrogels, injectable hydrogels have received much attention because of their simple implantation procedure with limited invasiveness and ability to change as per the irregular wound area. Recently, diverse injectable self-healing hydrogel systems embedded with PSs have been formulated for their prominent applications in regenerative medicine. More importantly, the rapid gelation time of injectable hydrogels protects the embedded PSs from diffusion and coagulation during the injection on the wound site [150]. Generally, the injectable hydrogels were prepared via physical or chemical crosslinking of polymers. While physically cross-linked hydrogels are safer due to the absence of toxic solvents and initiators, chemically cross-linked hydrogels are assumed to have better mechanical properties.

A hybrid supramolecular hydrogel was prepared by self-assembling an amphiphilic peptide (Fmoc-FF) and a fullerene derivative (C_{60}-PTC). The incorporation of C_{60}-PTC improved the mechanical properties of the hydrogel and allowed them to act as an injectable formulation. In addition, fullerene aggregation within the gel matrix was largely inhibited through the non-covalent interactions. Consequently, the APDT efficiency of the hybrid supramolecular hydrogel was highly improved compared to that of C_{60}-PTC alone [151]. The rhodamine-based PS with aggregation-inducing emission (AIE) effect was mixed with Carbomer 940 to prepare an antibacterial hydrogel dressing. The rhodamine-PS combined injectable hydrogel possesses excellent APDT performance, and promotes the healing of MRSA-infected wounds in mice due to its adhesiveness and moisture conditions [152]. Further, using polyphenol tannic acid as cross-linking agent significantly expands the mechanical strength of the injectable hydrogels [153]. Zhang et al. developed a physical/chemical double-crosslinked hydrogel based on dopamine-modified HA, Zr-based porphyrinic MOF-loaded BP nanosheets, and Fe^{3+} ions. The dopamine-modified HA and Fe^{3+} ions could form the dynamic physical cross-linked networks. Addition of Zr-based porphyrinic MOF-loaded BP nanosheets could generate ROS under 660 nm laser irradiation, which promoted the oxidative coupling of dopamine to form the chemical crosslinker within the hydrogel matrix. The as-obtained injectable hydrogel exhibited good APDT and APTT effects for effective sterilization [154]. Recently, a self-healing hydrogel consisting of PEG diamine, oxidized dextran (ODex), and amine-terminated PEG-functionalized CuS NPs was developed via Schiff base reactions. The CuS NPs-reinforced hydrogels endowed with good APTT and APDT performances under NIR laser irradiation to eradicate colonized bacteria effectively. In addition, the hydrogels can continuously release Cu^{2+}, promote the

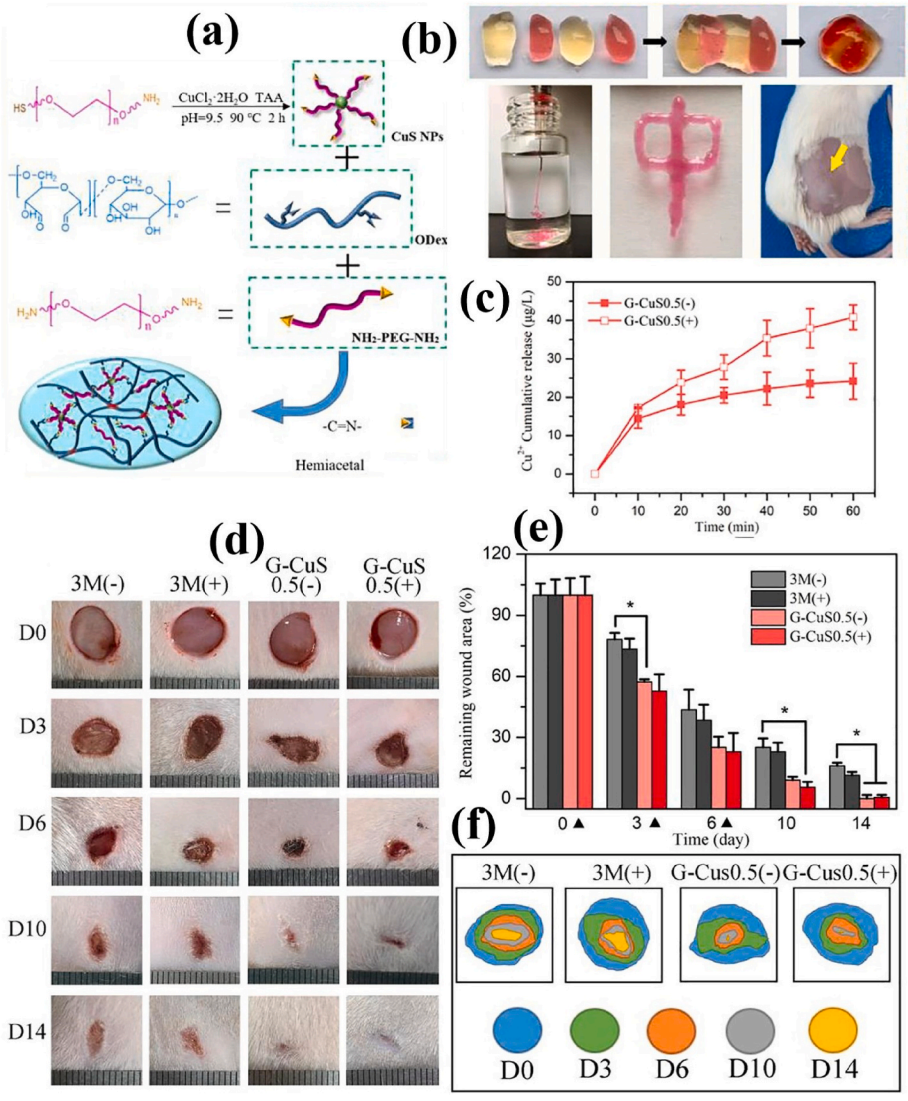

Fig. 12. (a) Illustration of the formation of CuS-integrated hydrogel; **(b)** Self-healing and injectable abilities of the CuS-integrated hydrogel; **(c)** Cu^{2+} cumulative release from hydrogel into PBS at 37 °C for 60 min with (+) and without (−) 808 nm laser irradiation (n = 3); **(d)** Photographs of wound area, **(e)** relative percentage of wound closure, and **(f)** illustration of wound healing progress after treated with 3 M dressing and CuS-integrated hydrogel. Reprinted with permission [155], Copyright © 2021, Elsevier.

proliferation of fibroblast cells and vascular endothelial cells, and ultimately expedite the wound healing process (Fig. 12a–f) [155]. These strategies take full advantage of the hydrogel characteristics to improve the clinical applicability of the PSs.

5.2.2. *Stimuli-responsive hydrogels*

An ideal hydrogel should be customized for APDT combined wound healing applications with improved mechanical, self-healable, stimuli-responsive, and on-demand reversible gelation properties. Especially, hydrogels with stimuli-responsive features such as temperature and pH would be more appropriate in APDT [156]. However, the covalently cross-linked hydrogels are more challenging to achieve without polymer degradation. In addition, these hydrogels lack targetability and cannot sense a microbial presence in the environment. Therefore, the wounded area pH has become crucial in formulating target-specific and stimuli-responsive hydrogels. Compared to native pH, the wound fluid remains acidic due to the release of organic acids and microbial infection [157–160].

The reversible swelling-shrinking behavior of hydrogels can be triggered upon pH variation, which could provoke the immune system and accelerate the wound healing process. Mao et al. reported the carboxymethyl cellulose (CMC) hydrogel consisting of Ag/Ag@AgCl/ZnO nanostructures via in situ chemical reduction and precipitation. The Ag/Ag@AgCl nanostructures enhanced ZnO's photocatalytic and antibacterial activity due to improved ROS generation by visible light. The hybrid CMC hydrogel showed a good swelling-shrinking effect according to pH change in the biological microenvironment. The electrostatic repulsive force caused hydrogel swelling at pH 7.4 and quickly shrinking at pH 2, due to protonation of the carboxylate groups in CMC. The release profiles of both Ag^{+} and Zn^{2+} showed initial burst release followed by sustained release after 3 days. *In vivo* results showed that Ag^{+} and Zn^{2+} released from the hydrogel stimulated the immune function to produce a large number of white blood cells and neutrophils (2–4 times more than the control), thereby producing the synergistic antibacterial effects and accelerated wound healing (Fig. 13a–e) [161].

Natural polymer lignin was used as a reducing, capping, and stabilizing agent to synthesize the Au and Ag nanocomposites. RB was then reacted with the hydroxyl groups of lignin to form the lignin-based photodynamic nanoconjugates. The obtained nanoconjugates were further loaded into the poly(acrylic acid) (PAA) matrix, forming a pH-responsive photodynamic antimicrobial hydrogel. The hydrogels proved to be highly stable at neutral and alkaline pH (7.4 and 9.1,

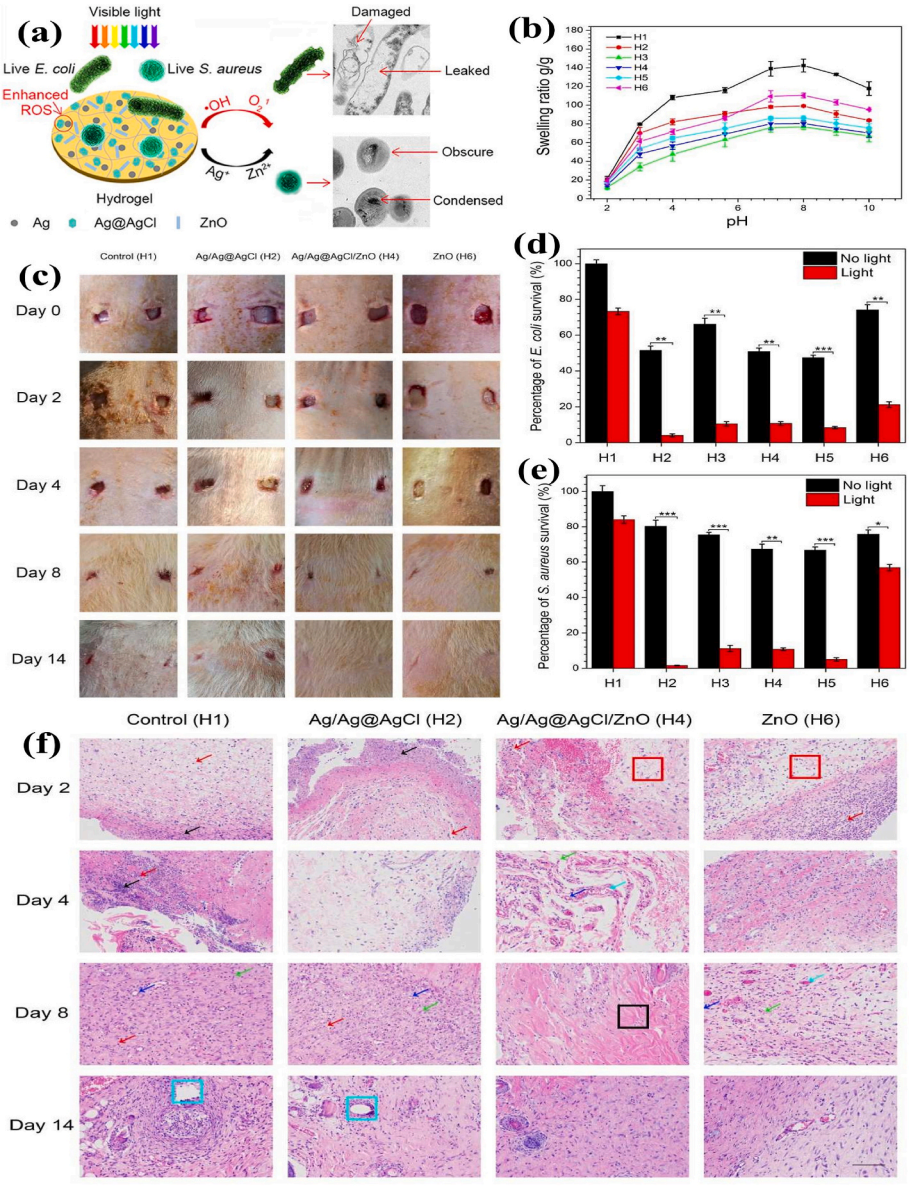

Fig. 13. **(a)** Schematic diagram of Ag/Ag@AgCl/ZnO hydrogel as a dressing for enhanced antibacterial activity; **(b)** Swelling behavior of the hydrogels at different pH values; **(c)** *In vivo* antibacterial effect of the hydrogel on *S. aureus*-induced wound infections; **(d and e)** Bacterial killing efficiency of Ag/Ag@AgCl/ZnO hydrogel against *E. coli* and *S. aureus* under simulated sunlight for 20 min (n = 3); **(f)** The immunology of histological images of the skin tissue samples on rats' wounds after treating with hydrogels and staining with hematoxylin-eosin (H&E). Reprinted with permission [161], Copyright © 2017, American Chemical Society.

respectively). Upon exposure to lower pH of 5.5, the breakdown of H-bonds inside the hydrogel causes hydrogel degradation and releases the nanoconjugates. The hydrogel could find applications as targeted therapeutics for wound healing [162].

A thermosensitive hydrogel with sol-gel transition potential at skin temperature (34 °C) can fill wound cavities and repair traumatic injuries with minimal side effects. Various amphiphilic block copolymers, such as polyethylene oxide (PEO)–polypropylene oxide (PPO) copolymers (PEO–PPO–PEO, also termed Poloxamers and Pluronics), were explored for the preparation of thermosensitive hydrogel with tolerability, and low-level irritancy and toxicity. For topical application, Poloxamer 407 (P407), a non-ionic triblock copolymer consisting of a central hydrophobic block of PPO flanked by two hydrophilic PEO blocks (PEO_{100}-PPO_{65}-PEO_{100}), has been the most studied thermosensitive gelling agent. The P407-based (15–20%) thermosensitive hydrogels combined with Carbopol® 934P (0.15–0.25%) have been formed to deliver MB. A considerable amount of MB (≥60%) was released from the hydrogels in 2 h, which is an adequate period for APDT in real life without much depletion of PS. The stimuli-responsive hydrogel could effectively kill three clinical MRSA strains under light irradiation [163]. PSs integrated hydrogels with better biodegradability, swelling behavior, and improved tissue adhesiveness provides hemostatic, photo-induced bacterial sterilization and accelerate wound healing properties. Continuous self-oxygenated PDT hydrogels improves biofilm hypoxia relief, inflammation control, immune-bio modulation, and vascularization. Moreover, the smart light activable hydrogels help in wound microenvironment responsive PDI action, real-time monitoring and modulating bacterial QS, and promote angiogenesis and anti-oxidant properties.

6. Summary and future direction

The ability to integrate porphyrin- and non-porphyrin-based PSs in a polymer matrix boosted the prospect of obtaining high ROS-producing systems for practical APDT applications, according to the findings described in this review. Polymer-based phototherapeutic materials have been demonstrated as a feasible approach for addressing the limitations of traditional PSs. The current state of extant PSs and their hybrid combinations with natural and synthetic polymers produce engineered functional materials, such as composites, surface coatings, films, scaffolds, and hydrogels with improved PDI action against bacterial pathogens. PSs were integrated into polymeric systems by functionalization, conjugation, encapsulation, and other non-covalent interactions. In most investigations, PSs embedded in polymeric materials outperformed free PSs in ROS generation and PDI action. Furthermore, these active systems aid in the PDI of microorganisms, biofilm eradication, imaging, diagnostics and wound healing.

Following a vast selection of recent scientific reports, polymer-PS combinational ventures are promising for APDT because they can use NIR radiation for deep tissues penetration and triggering of high ROS production. Preliminary *in vitro* testing revealed that the natural and synthetic polymeric systems combined with PSs had a significant photo-killing rate when exposed to light. The following elements support the enhanced APDT effect: i) When PSs are coupled with polymeric systems, their solubility, hydrophilicity, biocompatibility, and ROS generation efficiency are improved; ii) Combining PSs with cationic polymers boosts their capacity to bind to Gram-negative bacteria on the cell surface; iii) Combining high NIR absorption agents (or photothermal agents) with PSs in biocompatible polymers results in a synergistic photo-killing impact on planktonic bacteria and associated biofilms.

Experiments on several animal models revealed excellent APDT, wound healing and pharmacokinetics, paving the way for additional pre-clinical studies. Compared to anticancer PDT drugs, only a few clinical trials using polymer-based APDT systems have been performed. All these engineered polymeric materials need to be enriched further with essential additives to overcome certain limitations in clinical translation. More combinational APDT polymeric matrices must be formulated with long-term $^3PS^*$ and ISC elevation with increased ROS production. Multimodal therapeutic strategies can be acquired for synergetic actions by integrating new generation drug candidates such as nanozymes, nanoreactors, and natural products. The optimal PDT combination therapy will penetrate deep tissue infections, exhibit synergistic effectiveness, promote antibacterial immune responses, improve intracellular enzymatic activity, and alleviate hypoxia. Based on constructive analyses of the reported studies, it is likely to conclude that the combinatorial therapeutic approaches with distinct polymer-based functional materials would bring even more exciting advantages to APDT and vastly broaden the therapeutic alternatives for other infectious illnesses. Hence, more studies to identify the plausible mechanism, real-time monitoring of APDT action, theragnostic abilities, and the clinical implications of polymer-PSs hybrids should be demonstrated to translate test data to patient outcomes.

Ethics approval and consent to participate

Not applicable in present case.

Declaration of competing interest

The authors declare that they have no known competing financial interests or personal relationships that could have appeared to influence the work reported in this paper.

Acknowledgments

This research was supported by the National Natural Science Foundation of China (21504072, 51741304 and 52073234), Natural Science Foundation of Chongqing (cstc2019jcyj-msxmX0363), Innovation Teams in Colleges and Universities of Chongqing (CXQT20005), the innovation platform for Academicians of Hainan Province and Chongqing Engineering Research Center for Micro-Nano Biomedical Materials and Devices.

References

[1] Y. Wang, Y. Jin, W. Chen, J. Wang, H. Chen, L. Sun, et al., Construction of nanomaterials with targeting phototherapy properties to inhibit resistant bacteria and biofilm infections, Chem. Eng. J. 358 (2019) 74–90.
[2] R.J. Fair, Y. Tor, Antibiotics and bacterial resistance in the 21st century, Perspect. Med. Chem. 6 (2014). PMC. S14459.
[3] U. Hofer, The cost of antimicrobial resistance, Nat. Rev. Microbiol. 17 (2019) 3.
[4] S.L. Chua, Y. Liu, J.K.H. Yam, Y. Chen, R.M. Vejborg, B.G.C. Tan, et al., Dispersed cells represent a distinct stage in the transition from bacterial biofilm to planktonic lifestyles, Nat. Commun. 5 (2014) 1–12.
[5] W. Geneva, WHO's First Global Report on Antibiotic Resistance Reveals Serious, Worldwide Threat to Public Health, 2014.
[6] Control CfD, Prevention, Antibiotic Resistance Threats in the United States, 2019, US Department of Health and Human Services, Centres for Disease Control and ..., 2019.
[7] J. O'Neill, Tackling Drug-Resistant Infections Globally: Final Report and Recommendations, 2016.
[8] Y. Ren, H. Liu, X. Liu, Y. Zheng, Z. Li, C. Li, et al., Photoresponsive materials for antibacterial applications, Cell Rep Phys Sci 1 (2020), 100245.
[9] L. Li, Y. Liu, P. Hao, Z. Wang, L. Fu, Z. Ma, et al., PEDOT nanocomposites mediated dual-modal photodynamic and photothermal targeted sterilization in both NIR I and II window, Biomaterials 41 (2015) 132–140.
[10] G. Wei, G. Yang, Y. Wang, H. Jiang, Y. Fu, G. Yue, et al., Phototherapy-based combination strategies for bacterial infection treatment, Theranostics 10 (2020), 12241.
[11] K. Bilici, N. Atac, A. Muti, I. Baylam, O. Dogan, A. Sennaroglu, et al., Broad spectrum antibacterial photodynamic and photothermal therapy achieved with indocyanine green loaded SPIONs under near infrared irradiation, Biomater. Sci. 8 (2020) 4616–4625.
[12] Z. Yuan, C. Lin, Y. He, B. Tao, M. Chen, J. Zhang, et al., Near-infrared light-triggered nitric-oxide-enhanced photodynamic therapy and low-temperature photothermal therapy for biofilm elimination, ACS Nano 14 (2020) 3546–3562.
[13] J. Zhang, R.T. Zhou, H. Wang, X.Y. Jiang, H.Y. Wang, S.J. Yan, et al., Bacterial activation of surface-tethered antimicrobial peptides for the facile construction of a surface with self-defense, Appl. Surf. Sci. 497 (2019), 143780.

[14] F. Sperandio F, Y.-Y. Huang, M. R Hamblin, Antimicrobial photodynamic therapy to kill Gram-negative bacteria, Recent Pat. Anti-Infect. Drug Discov. 8 (2013) 108–120.

[15] Q. Jia, Q. Song, P. Li, W. Huang, Rejuvenated photodynamic therapy for bacterial infections, Advanced healthcare materials 8 (2019), 1900608.

[16] Q. Deng, P. Sun, L. Zhang, Z. Liu, H. Wang, J. Ren, et al., Porphyrin MOF dots–based, function-adaptive nanoplatform for enhanced penetration and photodynamic eradication of bacterial biofilms, Adv. Funct. Mater. 29 (2019), 1903018.

[17] A.-G. Niculescu, A.M. Grumezescu, Photodynamic therapy—an up-to-date review, Appl. Sci. 11 (2021) 3626.

[18] V. Pérez-Laguna, Y. Gilaberte, M.I. Millán-Lou, M. Agut, S. Nonell, A. Rezusta, et al., A combination of photodynamic therapy and antimicrobial compounds to treat skin and mucosal infections: a systematic review, Photochem. Photobiol. Sci. 18 (2019) 1020–1029.

[19] J. Chen, T. Fan, Z. Xie, Q. Zeng, P. Xue, T. Zheng, et al., Advances in nanomaterials for photodynamic therapy applications: status and challenges, Biomaterials 237 (2020), 119827.

[20] N.S. Soukos, L.A. Ximenez-Fyvie, M.R. Hamblin, S.S. Socransky, T. Hasan, Targeted antimicrobial photochemotherapy, Antimicrob. Agents Chemother. 42 (1998) 2595–2601.

[21] N. Kashef, M.R. Hamblin, Can microbial cells develop resistance to oxidative stress in antimicrobial photodynamic inactivation? Drug Resist. Updates 31 (2017) 31–42.

[22] J. Tian, B. Huang, M.H. Nawaz, W. Zhang, Recent advances of multi-dimensional porphyrin-based functional materials in photodynamic therapy, Coord. Chem. Rev. 420 (2020), 213410.

[23] M. Lan, S. Zhao, W. Liu, C.S. Lee, W. Zhang, P. Wang, Photosensitizers for photodynamic therapy, Adv Healthc Mater 8 (2019), 1900132.

[24] S. Kwiatkowski, B. Knap, D. Przystupski, J. Saczko, E. Kędzierska, K. Knap-Czop, et al., Photodynamic therapy–mechanisms, photosensitizers and combinations, Biomed. Pharmacother. 106 (2018) 1098–1107.

[25] H. Abrahamse, M.R. Hamblin, New photosensitizers for photodynamic therapy, Biochem. J. 473 (2016) 347–364.

[26] J. Ghorbani, D. Rahban, S. Aghamiri, A. Teymouri, A. Bahador, Photosensitizers in antibacterial photodynamic therapy: an overview, Laser Ther. 27 (2018) 293–302.

[27] L. Sobotta, P. Skupin-Mrugalska, J. Piskorz, J. Mielcarek, Porphyrinoid photosensitizers mediated photodynamic inactivation against bacteria, Eur. J. Med. Chem. 175 (2019) 72–106.

[28] B.M. Amos-Tautua, S.P. Songca, O.S. Oluwafemi, Application of porphyrins in antibacterial photodynamic therapy, Molecules 24 (2019) 2456.

[29] M. Wainwright, D. Phoenix, S. Laycock, D. Wareing, P. Wright, Photobactericidal activity of phenothiazinium dyes against methicillin-resistant strains of Staphylococcus aureus, FEMS Microbiol. Lett. 160 (1998) 177–181.

[30] J. Zhang, C. Jiang, J.P.F. Longo, R.B. Azevedo, H. Zhang, L.A. Muehlmann, An updated overview on the development of new photosensitizers for anticancer photodynamic therapy, Acta Pharm. Sin. B 8 (2018) 137–146.

[31] Z. Chai, F. Zhang, B. Liu, X. Chen, X. Meng, Antibacterial mechanism and preservation effect of curcumin-based photodynamic extends the shelf life of fresh-cut pears, Lebensm. Wiss. Technol. 142 (2021), 110941.

[32] J. Hao, Z.S. Lu, C.M. Li, L.Q. Xu, A maltoheptaose-decorated BODIPY photosensitizer for photodynamic inactivation of Gram-positive bacteria, New J. Chem. 43 (2019) 15057–15065.

[33] S.S. Lucky, K.C. Soo, Y. Zhang, Nanoparticles in photodynamic therapy, Chem. Rev. 115 (2015) 1990–2042.

[34] M.M. Kim, A. Darafsheh, Light sources and dosimetry techniques for photodynamic therapy, Photochem. Photobiol. 96 (2020) 280–294.

[35] Y. Nitzan, S. Gozhansky, Z. Malik, Effect of photoactivated hematoporphyrin derivative on the viability of Staphylococcus aureus, Curr. Microbiol. 8 (1983) 279–284.

[36] M.R. Hamblin, T. Hasan, Photodynamic therapy: a new antimicrobial approach to infectious disease? Photochem. Photobiol. Sci. 3 (2004) 436–450.

[37] A.P. Castano, T.N. Demidova, M.R. Hamblin, Mechanisms in photodynamic therapy: part one—photosensitizers, photochemistry and cellular localization, Photodiagnosis Photodyn. Ther. 1 (2004) 279–293.

[38] M. Wainwright, T. Maisch, S. Nonell, K. Plaetzer, A. Almeida, G.P. Tegos, et al., Photoantimicrobials—are we afraid of the light? Lancet Infect. Dis. 17 (2017) e49–e55.

[39] M.M. Gois, C. Kurachi, E. Santana, EGdO. Mima, D.M.P. Spolidório, J.E.P. Pelino, et al., Susceptibility of Staphylococcus aureus to porphyrin-mediated photodynamic antimicrobial chemotherapy: an in vitro study, Laser Med. Sci. 25 (2010) 391–395.

[40] F. Vatansever, W. de Melo, P. Avci, D. Vecchio, M. Sadasivam, A. Gupta, 559 chandran R.; Karimi, M.; Parizotto, NA; Yin, R, FEMS (Fed. Eur. Microbiol. Soc.) Microbiol. Rev. 37 (2013) 955–989.

[41] M.F. Wu, M. Deichelbohrer, T. Tschernig, M.W. Laschke, N. Szentmáry, D. Hüttenberger, H.J. Foth, B. Seitz, M. Bischoff, Chlorin e6 mediated photodynamic inactivation for multidrug resistant Pseudomonas aeruginosa keratitis in mice in vivo, Sci. Rep. 7 (2017) 1–12.

[42] M. Terra-Garcia, C.M. De Souza, N.M.F. Gonçalves, A.H.C. Pereira, P.P. DeBarros, A.B. Borges, W. Miyakawa, J.F. Strixino, J.C. Junqueira, Antimicrobial effects of photodynamic therapy with Fotoenticine on *Streptococcus mutans* isolated from dental caries, Photodiagnosis Photodyn. Ther. 34 (2021), 102303.

[43] Y. Ren, H. Liu, X. Liu, Y. Zheng, Z. Li, C. Li, et al., Photoresponsive materials for antibacterial applications, Cell Reports Physical Science 1 (2020), 100245.

[44] M. Tim, Strategies to optimize photosensitizers for photodynamic inactivation of bacteria, J. Photochem. Photobiol. B Biol. 150 (2015) 2–10.

[45] A.V. Morales-de-Echegaray, L. Lin, B. Sivasubramaniam, A. Yermembetova, Q. Wang, N.S. Abutaleb, et al., Antimicrobial photodynamic activity of gallium-substituted haemoglobin on silver nanoparticles, Nanoscale 12 (2020) 21734–21742.

[46] S. Mahboob, R. Nivetha, K. Gopinath, C. Balalakshmi, K.A. Al-Ghanim, F. Al-Misned, et al., Facile synthesis of gold and platinum doped titanium oxide nanoparticles for antibacterial and photocatalytic activity: a photodynamic approach, Photodiagnosis Photodyn. Ther. 33 (2021), 102148.

[47] A. Golmohamadpour, B. Bahramian, M. Khoobi, M. Pourhajibagher, H. R. Barikani, A. Bahador, Antimicrobial photodynamic therapy assessment of three indocyanine green-loaded metal-organic frameworks against Enterococcus faecalis, Photodiagnosis Photodyn. Ther. 23 (2018) 331–338.

[48] X. Nie, C. Jiang, S. Wu, W. Chen, P. Lv, Q. Wang, et al., Carbon quantum dots: a bright future as photosensitizers for in vitro antibacterial photodynamic inactivation, J. Photochem. Photobiol. B Biol. 206 (2020), 111864.

[49] X. Wu, X. Jiang, T. Fan, Z. Zheng, Z. Liu, Y. Chen, et al., Recent advances in photodynamic therapy based on emerging two-dimensional layered nanomaterials, Nano Res. 13 (2020) 1485–1508.

[50] L. Wang, Y. Li, L. Zhao, Z. Qi, J. Gou, S. Zhang, et al., Recent advances in ultrathin two-dimensional materials and biomedical applications for reactive oxygen species generation and scavenging, Nanoscale 12 (2020) 19516–19535.

[51] T. Xie, Y. Qi, Y. Li, F. Zhang, W. Li, D. Zhong, et al., Ultrasmall Ga-ICG nanoparticles based gallium ion/photodynamic synergistic therapy to eradicate biofilms and against drug-resistant bacterial liver abscess, Bioact. Mater. 6 (2021) 3812–3823.

[52] Y. Liu, K. Ma, T. Jiao, R. Xing, G. Shen, X. Yan, Water-insoluble photosensitizer nanocolloids stabilized by supramolecular interfacial assembly towards photodynamic therapy, Sci. Rep. 7 (2017) 1–8.

[53] J. Zhang, F. An, Y. Li, C. Zheng, Y. Yang, X. Zhang, et al., Simultaneous enhanced diagnosis and photodynamic therapy of photosensitizer-doped perylene nanoparticles via doping, fluorescence resonance energy transfer, and antenna effect, Chem. Commun. 49 (2013) 8072–8074.

[54] M. Sharma, A. Dube, S.K. Majumder, Antibacterial photodynamic activity of photosensitizer-embedded alginate-pectin-carboxymethyl cellulose composite biopolymer films, Laser Med. Sci. 36 (2021) 763–772.

[55] C. Li, F. Lin, W. Sun, F.-G. Wu, H. Yang, R. Lv, et al., Self-assembled rose bengal-exopolysaccharide nanoparticles for improved photodynamic inactivation of bacteria by enhancing singlet oxygen generation directly in the solution, ACS Appl. Mater. Interfaces 10 (2018) 16715–16722.

[56] L. Mei, Y. Shi, F. Cao, X. Liu, X.-M. Li, Z. Xu, et al., PEGylated phthalocyanine-functionalized graphene oxide with ultrahigh-efficient photothermal performance for triple-mode antibacterial therapy, ACS Biomater. Sci. Eng. 7 (2021) 2638–2648.

[57] L.-Y. Guo, S.-Z. Yan, X. Tao, Q. Yang, Q. Li, T.-S. Wang, et al., Evaluation of hypocrellin A-loaded lipase sensitive polymer micelles for intervening methicillin-resistant Staphylococcus Aureus antibiotic-resistant bacterial infection, Mater. Sci. Eng. C 106 (2020), 110230.

[58] D. Hu, Y. Deng, F. Jia, Q. Jin, J. Ji, Surface charge switchable supramolecular nanocarriers for nitric oxide synergistic photodynamic eradication of biofilms, ACS Nano 14 (2019) 347–359.

[59] Q. Gao, D. Huang, Y. Deng, W. Yu, Q. Jin, J. Ji, et al., Chlorin e6 (Ce6)-loaded supramolecular polypeptide micelles with enhanced photodynamic therapy effect against Pseudomonas aeruginosa, Chem. Eng. J. 417 (2021), 129334.

[60] T. Zhou, Y. Yin, W. Cai, H. Wang, L. Fan, G. He, et al., A new antibacterial nano-system based on hematoporphyrin-carboxymethyl chitosan conjugate for enhanced photostability and photodynamic activity, Carbohydr. Polym. (2021), 118242.

[61] R. Zhang, Y. Li, M. Zhou, C. Wang, P. Feng, W. Miao, et al., Photodynamic chitosan nano-assembly as a potent alternative candidate for combating antibiotic-resistant bacteria, ACS Appl. Mater. Interfaces 11 (2019) 26711–26721.

[62] R. Jia, W. Tian, H. Bai, J. Zhang, S. Wang, J. Zhang, Sunlight-driven wearable and robust antibacterial coatings with water-soluble cellulose-based photosensitizers, Adv Healthc Mater 8 (2019), 1801591.

[63] C. Hu, F. Zhang, Q. Kong, Y. Lu, B. Zhang, C. Wu, R. Luo, Y. Wang, Synergistic chemical and photodynamic antimicrobial therapy for enhanced wound healing mediated by multifunctional light-responsive nanoparticles, Biomacromolecules 20 (2019) 4581–4592.

[64] S. Kirar, N.S. Thakur, J.K. Laha, U.C. Banerjee, Porphyrin functionalized gelatin nanoparticle-based biodegradable phototheranostics: potential tools for antimicrobial photodynamic therapy, ACS Appl. Bio Mater. 2 (2019) 4202–4212.

[65] J. Tang, B. Chu, J. Wang, B. Song, Y. Su, H. Wang, et al., Multifunctional nanoagents for ultrasensitive imaging and photoactive killing of Gram-negative and Gram-positive bacteria, Nat. Commun. 10 (2019) 4057.

[66] L. Sun, W. Jiang, H. Zhang, Y. Guo, W. Chen, Y. Jin, et al., Photosensitizer-loaded multifunctional chitosan nanoparticles for simultaneous in situ imaging, highly efficient bacterial biofilm eradication, and tumor ablation, ACS Appl. Mater. Interfaces 11 (2018) 2302–2316.

[67] Q. Wang, D. Zhang, J. Feng, T. Sun, C. Li, X. Xie, et al., Enhanced photodynamic inactivation for Gram-negative bacteria by branched polyethylenimine-containing nanoparticles under visible light irradiation, J. Colloid Interface Sci. 584 (2021) 539–550.

[68] F. Yu, C. Chen, G. Yang, Z. Ren, H. Cao, L. Zhang, et al., An acid-triggered porphyrin-based block copolymer for enhanced photodynamic antibacterial efficacy, Sci. China Chem. 64 (2021) 459–466.
[69] L. Yue, M. Zheng, I.M. Khan, Z. Wang, Chlorin e6 conjugated chitosan as an efficient photoantimicrobial agent, Int. J. Biol. Macromol. 183 (2021) 1309–1316.
[70] L. Mei, X. Gao, Y. Shi, C. Cheng, Z. Shi, M. Jiao, et al., Augmented graphene quantum dot-light irradiation therapy for bacteria-infected wounds, ACS Appl. Mater. Interfaces 12 (2020) 40153–40162.
[71] Y. Zhao, Z. Lu, X. Dai, X. Wei, Y. Yu, X. Chen, X. Zhang, C. Li, Glycomimetic-conjugated photosensitizer for specific *Pseudomonas aeruginosa* recognition and targeted photodynamic therapy, Bioconjugate Chem. 29 (2018) 3222–3230.
[72] R. Khan, M. Özkan, A. Khaligh, D. Tuncel, Water-dispersible glycosylated poly (2, 5′-thienylene) porphyrin-based nanoparticles for antibacterial photodynamic therapy, Photochem. Photobiol. Sci. 18 (2019) 1147–1155.
[73] P. Liu, L.Q. Xu, G. Xu, D. Pranantyo, K.-G. Neoh, E.-T. Kang, pH-sensitive theranostic nanoparticles for targeting bacteria with fluorescence imaging and dual-modal antimicrobial therapy, ACS Appl. Nano Mater. 1 (2018) 6187–6196.
[74] L.G. Ning, P. Liu, B. Wang, C.M. Li, E.-T. Kang, Z.S. Lu, et al., Hydrothermal derived protoporphyrin IX nanoparticles for inactivation and imaging of bacteria strains, J. Colloid Interface Sci. 549 (2019) 72–79.
[75] Y.-D. Sun, Y.-X. Zhu, X. Zhang, H.-R. Jia, Y. Xia, F.-G. Wu, Role of cholesterol conjugation in the antibacterial photodynamic therapy of branched polyethylenimine-containing nanoagents, Langmuir 35 (44) (2019) 14324–14331.
[76] L.L.R. Cavalcante, A.C. Tedesco, L.A.U. Takahashi, F.A. Curylofo-Zotti, A. E. Souza-Gabriel, S.A.M. Corona, Conjugate of chitosan nanoparticles with chloroaluminium phthalocyanine: synthesis, characterization and photoinactivation of Streptococcus mutans biofilm, Photodiagnosis Photodyn. Ther. 30 (2020), 101709.
[77] Q. Wang, D. Zhang, J. Feng, T. Sun, C. Li, X. Xie, et al., Enhanced photodynamic inactivation for Gram-negative bacteria by branched polyethylenimine-containing nanoparticles under visible light irradiation, J. Colloid Interface Sci. 584 (2021) 539–550.
[78] Y. Liu, H.C. van der Mei, B. Zhao, Y. Zhai, T. Cheng, Y. Li, et al., Eradication of multidrug-resistant staphylococcal infections by light-activatable micellar nanocarriers in a murine model, Adv. Funct. Mater. 27 (2017), 1701974.
[79] X. Hou, L. Yang, J. Liu, Y. Zhang, L. Chu, C. Ren, et al., Silver-decorated, light-activatable polymeric antimicrobials for combined chemo-photodynamic therapy of drug-resistant bacterial infection, Biomater. Sci. 8 (2020) 6350–6361.
[80] N. Wijesiri, T. Ozkaya-Ahmadov, P. Wang, J. Zhang, H. Tang, X. Yu, et al., Photodynamic inactivation of multidrug-resistant Staphylococcus aureus using hybrid photosensitizers based on amphiphilic block copolymer-functionalized gold nanoparticles, ACS Omega 2 (2017) 5364–5369.
[81] R. Ding, X. Yu, P. Wang, J. Zhang, Y. Zhou, X. Cao, et al., Hybrid photosensitizer based on amphiphilic block copolymer stabilized silver nanoparticles for highly efficient photodynamic inactivation of bacteria, RSC Adv. 6 (2016) 20392–20398.
[82] R. Sadowski, M. Strus, M. Buchalska, P.B. Heczko, W. Macyk, Visible light induced photocatalytic inactivation of bacteria by modified titanium dioxide films on organic polymers, Photochem. Photobiol. Sci. 14 (2015) 514–519.
[83] X. Dong, L. Ge, D.I.A. Rabe, O.O. Mohammed, P. Wang, Y. Tang, et al., Photoexcited state properties and antibacterial activities of carbon dots relevant to mechanistic features and implications, Carbon 170 (2020) 137–145.
[84] K. Zhou, X. Qiu, L. Xu, G. Li, B. Rao, B. Guo, et al., Poly (selenoviologen)-assembled upconversion nanoparticles for low-power single-NIR light-triggered synergistic photodynamic and photothermal antibacterial therapy, ACS Appl. Mater. Interfaces 12 (2020) 26432–26443.
[85] X. Zeng, Y. Liu, Y. Xia, M.H. Uddin, D. Xia, D.T. McCarthy, et al., Cooperatively modulating reactive oxygen species generation and bacteria-photocatalyst contact over graphitic carbon nitride by polyethylenimine for rapid water disinfection, Appl. Catal. B Environ. 274 (2020), 119095.
[86] C. Wang, Y. Xiao, W. Zhu, J. Chu, J. Xu, H. Zhao, F. Shen, R. Peng, Z. Liu, Photosensitizer-modified MnO2 nanoparticles to enhance photodynamic treatment of abscesses and boost immune protection for treated mice, Small 16 (2020), 2000589.
[87] W. Liu, Y. Zhang, W. You, J. Su, S. Yu, T. Dai, et al., Near-infrared-excited upconversion photodynamic therapy of extensively drug-resistant Acinetobacter baumannii based on lanthanide nanoparticles, Nanoscale 12 (2020) 13948–13957.
[88] B. Zhou, X. Sun, B. Dong, S. Yu, L. Cheng, S. Hu, et al., Antibacterial PDT nanoplatform capable of releasing therapeutic gas for synergistic and enhanced treatment against deep infections, Theranostics 12 (2022) 2580.
[89] T. Li, Y. Zhao, K. Matthews, J. Gao, J. Hao, S. Wang, et al., Antibacterial activity against Staphylococcus aureus of curcumin-loaded chitosan spray coupled with photodynamic treatment, LWT (Lebensm.-Wiss. & Technol.) 134 (2020), 110073.
[90] A. Severyukhina, N. Petrova, A. Yashchenok, D. Bratashov, K. Smuda, I. Mamonova, et al., Light-induced antibacterial activity of electrospun chitosan-based material containing photosensitizer, Mater. Sci. Eng. C 70 (2017) 311–316.
[91] W. Tong, Y. Xiong, S. Duan, X. Ding, F.-J. Xu, Phthalocyanine functionalized poly (glycidyl methacrylate) nano-assemblies for photodynamic inactivation of bacteria, Biomater. Sci. 7 (2019) 1905–1918.
[92] A.M. Malacrida, V.H.C. Dias, A.F. Silva, A.R. Dos Santos, G.B. Cesar, E. Bona, et al., Hypericin-mediated photoinactivation of polymeric nanoparticles against Staphylococcus aureus, Photodiagnosis Photodyn. Ther. 30 (2020), 101737.
[93] M.H. Staegemann, S. Grafe, B. Gitter, K. Achazi, E. Quaas, R. Haag, et al., Hyperbranched polyglycerol loaded with (zinc-) porphyrins: photosensitizer release under reductive and acidic conditions for improved photodynamic therapy, Biomacromolecules 19 (2018) 222–238.
[94] S. Wang, Y. Fang, Z. Zhang, Q. Jin, J. Ji, Bacterial infection microenvironment sensitive prodrug micelles with enhanced photodynamic activities for infection control, Colloid Interface Sci Commun 40 (2021), 100354.
[95] J. Chen, J. Shan, Y. Xu, P. Su, L. Tong, L. Yuwen, et al., Polyhedral oligomeric silsesquioxane (POSS)-based cationic conjugated oligoelectrolyte/porphyrin for efficient energy transfer and multiamplified antimicrobial activity, ACS Appl. Mater. Interfaces 10 (2018) 34455–34463.
[96] C.R. Arciola, D. Campoccia, L. Montanaro, Implant infections: adhesion, biofilm formation and immune evasion, Nat. Rev. Microbiol. 16 (2018) 397–409.
[97] C.R. Arciola, D. Campoccia, P. Speziale, L. Montanaro, J.W. Costerton, Biofilm formation in Staphylococcus implant infections. A review of molecular mechanisms and implications for biofilm-resistant materials, Biomaterials 33 (2012) 5967–5982.
[98] P. Sautrot-Ba, A. Contreras, S.A. Andaloussi, T. Coradin, C. Hélary, N. Razza, M. Sangermano, P.E. Mazeran, J.P. Malval, D.L. Versace, Eosin-mediated synthesis of polymer coatings combining photodynamic inactivation and antimicrobial properties, J. Mater. Chem. B 5 (2017) 7572–7582.
[99] L. Tan, J. Li, X. Liu, Z. Cui, X. Yang, S. Zhu, Z. Li, X. Yuan, Y. Zheng, K.W. Yeung, Rapid biofilm eradication on bone implants using red phosphorus and near-infrared light, Adv. Mater. 30 (2018), 1801808.
[100] T. Zhou, Y. Zhu, X. Li, X. Liu, K.W. Yeung, S. Wu, X. Wang, Z. Cui, X. Yang, P. K. Chu, Surface functionalization of biomaterials by radical polymerization, Prog. Mater. Sci. 83 (2016) 191–235.
[101] M. Hu, Y. Ju, K. Liang, T. Suma, J. Cui, F. Caruso, Void engineering in metal–organic frameworks via synergistic etching and surface functionalization, Adv. Funct. Mater. 26 (2016) 5827–5834.
[102] S. Wang, C. Duan, W. Yang, X. Gao, J. Shi, J. Kang, Y. Deng, X.L. Shi, Z.G. Chen, Two-dimensional nanocoating-enabled orthopedic implants for bimodal therapeutic applications, Nanoscale 12 (2020) 11936–11946.
[103] H. Lee, S.M. Dellatore, W.M. Miller, P.B. Messersmith, Mussel-inspired surface chemistry for multifunctional coatings, Science 318 (2007) 426–430.
[104] C. Gao, Y. Wang, F. Han, Z. Yuan, Q. Li, C. Shi, W. Cao, P. Zhou, X. Xing, B. Li, Antibacterial activity and osseointegration of silver-coated poly (ether ether ketone) prepared using the polydopamine-assisted deposition technique, J. Mater. Chem. B 5 (2017) 9326–9336.
[105] P. Yang, F. Zhu, Z. Zhang, Y. Cheng, Z. Wang, Y. Li, Stimuli-responsive polydopamine-based smart materials, Chem. Soc. Rev. 50 (2021) 8319–8343.
[106] J. Zeng, Y. Wang, Z. Sun, H. Chang, M. Cao, J. Zhao, et al., A novel biocompatible PDA/IR820/DAP coating for antibiotic/photodynamic/photothermal triple therapy to inhibit and eliminate Staphylococcus aureus biofilm, Chem. Eng. J. 394 (2020), 125017.
[107] X. Xie, C. Mao, X. Liu, L. Tan, Z. Cui, X. Yang, et al., Tuning the bandgap of photo-sensitive polydopamine/Ag3PO4/graphene oxide coating for rapid, noninvasive disinfection of implants, ACS Cent. Sci. 4 (2018) 724–738.
[108] X. Xie, C. Mao, X. Liu, Y. Zhang, Z. Cui, X. Yang, et al., Synergistic bacteria killing through photodynamic and physical actions of graphene oxide/Ag/collagen coating, ACS Appl. Mater. Interfaces 9 (2017) 26417–26428.
[109] S. Wang, C. Duan, W. Yang, X. Gao, J. Shi, J. Kang, et al., Two-dimensional nanocoating-enabled orthopedic implants for bimodal therapeutic applications, Nanoscale 12 (2020) 11936–11946.
[110] J. Zhang, X. Gao, D. Ma, S. He, B. Du, W. Yang, et al., Copper ferrite heterojunction coatings empower polyetheretherketone implant with multi-modal bactericidal functions and boosted osteogenicity through synergistic photo/Fenton-therapy, Chem. Eng. J. 422 (2021), 130094.
[111] Z. Yuan, B. Tao, Y. He, C. Mu, G. Liu, J. Zhang, et al., Remote eradication of biofilm on titanium implant via near-infrared light triggered photothermal/photodynamic therapy strategy, Biomaterials 223 (2019), 119479.
[112] Z. Feng, X. Liu, L. Tan, Z. Cui, X. Yang, Z. Li, et al., Electrophoretic deposited stable chitosan@ MoS2 coating with rapid in situ bacteria-killing ability under dual-light irradiation, Small 14 (2018), 1704347.
[113] Y. He, J. Leng, K. Li, K. Xu, C. Lin, Z. Yuan, et al., A multifunctional hydrogel coating to direct fibroblast activation and infected wound healing via simultaneously controllable photobiomodulation and photodynamic therapies, Biomaterials 278 (2021), 121164.
[114] Y. Li, X. Liu, B. Li, Y. Zheng, Y. Han, D-f Chen, et al., Near-infrared light triggered phototherapy and immunotherapy for elimination of methicillin-resistant Staphylococcus aureus biofilm infection on bone implant, ACS Nano 14 (2020) 8157–8170.
[115] A. Severyukhina, N. Petrova, K. Smuda, G. Terentyuk, B. Klebtsov, R. Georgieva, et al., Photosensitizer-loaded electrospun chitosan-based scaffolds for photodynamic therapy and tissue engineering, Colloids Surf. B Biointerfaces 144 (2016) 57–64.
[116] G. Kasi, S. Gnanasekar, K. Zhang, E.T. Kang, L.Q. Xu, Polyurethane-based composites with promising antibacterial properties, J. Appl. Polym. Sci. 139 (2022), 52181.
[117] A.J. Naik, S. Ismail, C. Kay, M. Wilson, I.P. Parkin, Antimicrobial activity of polyurethane embedded with methylene blue, toluidene blue and gold nanoparticles against *Staphylococcus aureus*; illuminated with white light, Mater. Chem. Phys. 129 (2011) 446–450.
[118] A.M. Ferreira, I. Carmagnola, V. Chiono, P. Gentile, L. Fracchia, C. Ceresa, G. Georgiev, G. Ciardelli, Surface modification of poly (dimethylsiloxane) by two-

step plasma treatment for further grafting with chitosan–Rose Bengal photosensitizer, Surf. Coating. Technol. 223 (2013) 92–97.
[119] M. Merchán, T.S. Ouk, P. Kubát, K. Lang, C. Coelho, V. Verney, S. Commereuc, F. Leroux, V. Sol, C. Taviot-Guého, Photostability and photobactericidal properties of porphyrin-layered double hydroxide–polyurethane composite films, J. Mater. Chem. B 1 (2013) 139–2146.
[120] S.K. Sehmi, S. Noimark, J.C. Bear, W.J. Peveler, M. Bovis, E. Allan, A. J. MacRobert, I.P. Parkin, Lethal photosensitisation of *Staphylococcus aureus* and *Escherichia coli* using crystal violet and zinc oxide-encapsulated polyurethane, J. Mater. Chem. B 3 (2015) 6490–6500.
[121] S. Noimark, E. Salvadori, R. Gómez-Bombarelli, A.J. MacRobert, I.P. Parkin, C. W. Kay, Comparative study of singlet oxygen production by photosensitiser dyes encapsulated in silicone: towards rational design of anti-microbial surfaces, Phys. Chem. Chem. Phys. 18 (2016) 28101–28109.
[122] S. Noimark, J. Weiner, N. Noor, E. Allan, C.K. Williams, M.S.P. Shaffer, et al., Dual-mechanism antimicrobial polymer–ZnO nanoparticle and crystal violet-encapsulated silicone, Adv. Funct. Mater. 25 (2015) 1367–1373.
[123] Mr Kovacova, Z.M. Markovic, P. Humpoicek, M. Micusik, H. svajdlenkova, A. Kleinova, et al., Carbon quantum dots modified polyurethane nanocomposite as effective photocatalytic and antibacterial agents, ACS Biomater. Sci. Eng. 4 (2018) 3983–3993.
[124] E.G. Owusu, A.J. MacRobert, I. Naasani, I.P. Parkin, E. Allan, E. Yaghini, Photoactivable polymers embedded with cadmium-free quantum dots and crystal violet: efficient bactericidal activity against clinical strains of antibiotic-resistant bacteria, ACS Appl. Mater. Interfaces 11 (2019) 12367–12378.
[125] H. Vögeling, N. Plenagl, B.S. Seitz, L. Duse, S.R. Pinnapireddy, E. Dayyoub, et al., Synergistic effects of ultrasound and photodynamic therapy leading to biofilm eradication on polyurethane catheter surfaces modified with hypericin nanoformulations, Mater. Sci. Eng. C 103 (2019), 109749.
[126] G. Wang, C. Yang, M. Shan, H. Jia, S. Zhang, X. Chen, et al., Synergistic poly (lactic acid) antibacterial surface combining superhydrophobicity for antiadhesion and chlorophyll for photodynamic therapy, Langmuir 38 (2022) 8987–8998.
[127] A.O. Pereira, I.M. Lopes, T.R. Silva, T.Q. Correa, R.T. Paschoalin, N.M. Inada, et al., Bacterial photoinactivation using PLGA electrospun scaffolds, ACS Appl. Mater. Interfaces 13 (2021) 31406–31417.
[128] T. Wang, H. Ke, S. Chen, J. Wang, W. Yang, X. Cao, et al., Porous protoporphyrin IX-embedded cellulose diacetate electrospun microfibers in antimicrobial photodynamic inactivation, Mater. Sci. Eng. C 118 (2021), 111502.
[129] P. Henke, J. Dolanský, P. Kubát, J. Mosinger, Multifunctional photosensitizing and biotinylated polystyrene nanofiber membranes/composites for binding of biologically active compounds, ACS Appl. Mater. Interfaces 12 (2020) 18792–18802.
[130] Q. Wang, W. Chen, Q. Zhang, R.A. Ghiladi, Q. Wei, Preparation of photodynamic P (MMA-co-MAA) composite nanofibers doped with MMT: a facile method for increasing antimicrobial efficiency, Appl. Surf. Sci. 457 (2018) 247–255.
[131] M.A. Castriciano, R. Zagami, M.P. Casaletto, B. Martel, M. Trapani, A. Romeo, et al., Poly (carboxylic acid)-cyclodextrin/anionic porphyrin finished fabrics as photosensitizer releasers for antimicrobial photodynamic therapy, Biomacromolecules 18 (2017) 1134–1144.
[132] J. Dong, R.A. Ghiladi, Q. Wang, Y. Cai, Q. Wei, Protoporphyrin IX conjugated bacterial cellulose via diamide spacer arms with specific antibacterial photodynamic inactivation against Escherichia coli, Cellulose 25 (2018) 1673–1686.
[133] L. Sun, L. Song, X. Zhang, R. Zhou, J. Yin, S. Luan, Poly (γ-glutamic acid)-based electrospun nanofibrous mats with photodynamic therapy for effectively combating wound infection, Mater. Sci. Eng. C 113 (2020), 110936.
[134] A. Contreras, M.J. Raxworthy, S. Wood, J.D. Schiffman, G. Tronci, Photodynamically active electrospun fibers for antibiotic-free infection control, ACS Appl. Bio Mater. 2 (2019) 4258–4270.
[135] S. Zhang, J. Ye, X. Liu, G. Wang, Y. Qi, T. Wang, et al., Dual Stimuli-Responsive smart fibrous membranes for efficient Photothermal/Photodynamic/Chemo-Therapy of Drug-Resistant bacterial infection, Chem. Eng. J. 432 (2022), 134351.
[136] H. Yang, Y. Liang, J. Wang, Q. Li, Q. Li, A. Tang, et al., Multifunctional wound dressing for rapid hemostasis, bacterial infection monitoring and photodynamic antibacterial therapy, Acta Biomater. 135 (2021) 179–190.
[137] Z. Fan, B. Liu, J. Wang, S. Zhang, Q. Lin, P. Gong, et al., A novel wound dressing based on Ag/graphene polymer hydrogel: effectively kill bacteria and accelerate wound healing, Adv. Funct. Mater. 24 (2014) 3933–3943.
[138] F. Bayat, A.R. Karimi, Design of photodynamic chitosan hydrogels bearing phthalocyanine-colistin conjugate as an antibacterial agent, Int. J. Biol. Macromol. 129 (2019) 927–935.
[139] A. Maleki, J. He, S. Bochani, V. Nosrati, M.-A. Shahbazi, B. Guo, Multifunctional photoactive hydrogels for wound healing acceleration, ACS Nano 15 (2021) 18895–18930.
[140] C. Mao, Y. Xiang, X. Liu, Z. Cui, X. Yang, Z. Li, et al., Repeatable photodynamic therapy with triggered signaling pathways of fibroblast cell proliferation and differentiation to promote bacteria-accompanied wound healing, ACS Nano 12 (2018) 1747–1759.
[141] Q. Wang, W. Qiu, M. Li, N. Li, X. Li, X. Qin, et al., Multifunctional hydrogel platform for biofilm scavenging and O2 generating with photothermal effect on diabetic chronic wound healing, J. Colloid Interface Sci. 617 (2022) 542–556.
[142] M. Li, X. Liu, L. Tan, Z. Cui, X. Yang, Z. Li, et al., Noninvasive rapid bacteria-killing and acceleration of wound healing through photothermal/photodynamic/copper ion synergistic action of a hybrid hydrogel, Biomater. Sci. 6 (2018) 2110–2121.
[143] Y. Xie, C. Gan, Z. Li, W. Liu, D. Yang, X. Qiu, Fabrication of a lignin-copper sulfide-incorporated PVA hydrogel with near-infrared-activated photothermal/photodynamic/peroxidase-like performance for combating bacteria and biofilms, ACS Biomater. Sci. Eng. 8 (2022) 560–569.
[144] Q. Ding, T. Sun, W. Su, X. Jing, B. Ye, Y. Su, et al., Bioinspired multifunctional black phosphorus hydrogel with antibacterial and antioxidant properties: a stepwise countermeasure for diabetic skin wound healing, Adv Healthc Mater (2022), 2102791.
[145] B. Mai, M. Jia, S. Liu, Z. Sheng, M. Li, Y. Gao, et al., Smart hydrogel-based DVDMS/bFGF nanohybrids for antibacterial phototherapy with multiple damaging sites and accelerated wound healing, ACS Appl. Mater. Interfaces 12 (2020) 10156–10169.
[146] R. Tian, J. Liu, G. Dou, B. Lin, J. Chen, G. Yang, et al., Synergistic antibiosis with spatiotemporal controllability based on multiple-responsive hydrogel for infectious cutaneous wound healing, Smart Materials in Medicine 3 (2022) 304–314.
[147] H. Hu, D. Zhong, W. Li, X. Lin, J. He, Y. Sun, et al., Microalgae-based bioactive hydrogel loaded with quorum sensing inhibitor promotes infected wound healing, Nano Today 42 (2022), 101368.
[148] L. Yu, J. Ding, Injectable hydrogels as unique biomedical materials, Chem. Soc. Rev. 37 (2008) 1473–1481.
[149] Y. Yao, A. Zhang, C. Yuan, X. Chen, Y. Liu, Recent trends on burn wound care: hydrogel dressings and scaffolds, Biomater. Sci. 9 (2021) 4523–4540.
[150] Y. Xiang, C. Mao, X. Liu, Z. Cui, D. Jing, X. Yang, et al., Rapid and superior bacteria killing of carbon quantum dots/ZnO decorated injectable folic acid-conjugated PDA hydrogel through dual-light triggered ROS and membrane permeability, Small 15 (2019), 1900322.
[151] Y. Zhang, H. Zhang, Q. Zou, R. Xing, T. Jiao, X. Yan, An injectable dipeptide–fullerene supramolecular hydrogel for photodynamic antibacterial therapy, J. Mater. Chem. B 6 (2018) 7335–7342.
[152] S. Zeng, Z. Wang, C. Chen, X. Liu, Y. Wang, Q. Chen, et al., Construction of rhodamine-based AIE photosensitizer hydrogel with clinical potential for selective ablation of drug-resistant gram-positive bacteria in vivo, Adv Healthc Mater (2022), 2200837.
[153] F. Azadikhah, A.R. Karimi, Injectable photosensitizing supramolecular hydrogels: a robust physically cross-linked system based on polyvinyl alcohol/chitosan/tannic acid with self-healing and antioxidant properties, React. Funct. Polym. 173 (2022), 105212.
[154] Y. Zhang, H. Wu, P. Li, W. Liu, Y. Zhang, A. Dong, Dual-light-triggered in situ structure and function regulation of injectable hydrogels for high-efficient anti-infective wound therapy, Adv Healthc Mater 11 (2022), 2101722.
[155] L. Zhou, F. Chen, Z. Hou, Y. Chen, X. Luo, Injectable self-healing CuS nanoparticle complex hydrogels with antibacterial, anti-cancer, and wound healing properties, Chem. Eng. J. 409 (2021), 128224.
[156] M. Ma, Y. Zhong, X. Jiang, Thermosensitive and pH-responsive tannin-containing hydroxypropyl chitin hydrogel with long-lasting antibacterial activity for wound healing, Carbohydr. Polym. 236 (2020), 116096.
[157] J. Qu, X. Zhao, Y. Liang, T. Zhang, P.X. Ma, B. Guo, Antibacterial adhesive injectable hydrogels with rapid self-healing, extensibility and compressibility as wound dressing for joints skin wound healing, Biomaterials 183 (2018) 185–199.
[158] L. Zhang, Y. Zhou, D. Su, S. Wu, J. Zhou, J. Chen, Injectable, self-healing and pH responsive stem cell factor loaded collagen hydrogel as a dynamic bioadhesive dressing for diabetic wound repair, J. Mater. Chem. B 9 (2021) 5887–5897.
[159] N. Ninan, A. Forget, V.P. Shastri, N.H. Voelcker, A. Blencowe, Antibacterial and anti-inflammatory pH-responsive tannic acid-carboxylated agarose composite hydrogels for wound healing, ACS Appl. Mater. Interfaces 8 (2016) 28511–28521.
[160] K. Zhang, Q. Feng, Z. Fang, L. Gu, L. Bian, Structurally dynamic hydrogels for biomedical applications: Pursuing a fine balance between macroscopic stability and microscopic dynamics, Chem. Rev. 121 (2021) 11149–11193.
[161] C. Mao, Y. Xiang, X. Liu, Z. Cui, X. Yang, K.W.K. Yeung, et al., Photo-inspired antibacterial activity and wound healing acceleration by hydrogel embedded with Ag/Ag@ AgCl/ZnO nanostructures, ACS Nano 11 (2017) 9010–9021.
[162] S. Chandna, N.S. Thakur, R. Kaur, J. Bhaumik, Lignin–bimetallic nanoconjugate doped pH-responsive hydrogels for laser-assisted antimicrobial photodynamic therapy, Biomacromolecules 21 (2020) 3216–3230.
[163] B. Leung, P. Dharmaratne, W. Yan, B.C. Chan, C.B. Lau, K.-P. Fung, et al., Development of thermosensitive hydrogel containing methylene blue for topical antimicrobial photodynamic therapy, J. Photochem. Photobiol. B Biol. 203 (2020), 111776.